

# The impact of heterogeneous mixed siliciclastic–carbonate systems on CO<sub>2</sub> geological storage

**Pourmalek, A., Newell, A., Shariatipour, S. M. & Wood, A.**

Author post-print (accepted) deposited by Coventry University's Repository

**Original citation & hyperlink:**

Pourmalek, A, Newell, A, Shariatipour, SM & Wood, A 2022, 'The impact of heterogeneous mixed siliciclastic–carbonate systems on CO<sub>2</sub> geological storage', *Petroleum Geoscience*, vol. 28, no. 1.

<https://dx.doi.org/10.1144/petgeo2020-086>

DOI 10.1144/petgeo2020-086

ISSN 1354-0793

ESSN 2041-496X

Publisher: The Geological Society

**Copyright © and Moral Rights are retained by the author(s) and/ or other copyright owners. A copy can be downloaded for personal non-commercial research or study, without prior permission or charge. This item cannot be reproduced or quoted extensively from without first obtaining permission in writing from the copyright holder(s). The content must not be changed in any way or sold commercially in any format or medium without the formal permission of the copyright holders.**

**This document is the author's post-print version, incorporating any revisions agreed during the peer-review process. Some differences between the published version and this version may remain and you are advised to consult the published version if you wish to cite from it.**

# **The impact of heterogeneous mixed siliciclastic-carbonate systems on CO<sub>2</sub> geological storage**

Azadeh Pourmalek<sup>1</sup>, Andrew J. Newell<sup>2</sup>, Seyed M. Shariatipour<sup>1</sup>, Adrian M. Wood<sup>3</sup>

Fluid and Complex Systems Research Centre, Faculty of Engineering, Environment and Computing, Coventry University, CV1 2NL

British Geological Survey, Maclean Building, Wallingford, OX10 8BB

School of Energy, Construction and Environment, Coventry University, CV1 2LT

## **Abstract**

Three different outcrops are selected in this study, each representing a shallow marine system with varying heterogeneity provided by siliciclastic-carbonate mixing that may form a small or large stratigraphic trap. The impact of these styles of mixed facies on CO<sub>2</sub> storage is relatively poorly known. This study demonstrates the significance of these systems for safe CO<sub>2</sub> geological storage, as stratigraphic traps are likely to be a significant feature of many future storage sites. The three 3D models are based on the: 1. Grayburg Formation (US), which displays spatial permeability linked to variations in the mixture of siliciclastic-carbonate sediments; 2. Lorca Basin outcrop (Spain), which demonstrates the interfingering of clastic and carbonate facies; and 3. Bridport Sand Formation outcrop (UK), an example of a layered reservoir, which has thin carbonate-cemented horizons.

This study demonstrates that facies interplay and associated sediment heterogeneity have a varying effect on fluid flow, storage capacity and security. In the Grayburg Formation, storage security and capacity are not controlled by heterogeneity alone but influenced mainly by the permeability of each facies (i.e., permeability contrast), the degree of heterogeneity, and the relative permeability characteristic of the system. In the case of the Lorca Basin, heterogeneity through interfingering of the carbonate and clastic facies improved the storage security regardless of their permeability. For the Bridport Sand Formation, the existence of extended sheets of cemented carbonate contributed to storage security but not storage capacity, which depends on the continuity of the sheets. These mixed systems specially minimise the large buoyancy force that act on the top seal and reduce the reliance of the storage security on the overlying caprock. They also increase the contact area between injected CO<sub>2</sub> and brine, thereby promoting the CO<sub>2</sub> dissolution processes. Overall, mixed systems contribute to the safe storage of CO<sub>2</sub>.

## **Keywords**

Mixed siliciclastic-carbonate system, Carbon Capture and Storage, Geological CO<sub>2</sub> Storage

## 1. Introduction

Carbon capture and storage (CCS) is one of several measures that could be used to stabilize atmospheric CO<sub>2</sub> concentrations while still using fossil fuels (Orr 2009; Benson and Surles 2006; Ennis-King and Paterson 2005; IPCC 2005), as economies transition to more sustainable energy sources (IEA 2019). The storage element of CCS refers to CO<sub>2</sub> storage in geological media, mostly deep saline aquifers with high storage capacity (e.g., Pourmalek and Shariatipour 2019; Shariatipour et al. 2016b; Celia et al. 2015; Peters et al. 2015; Chadwick et al. 2008; Birkholzer et al. 2009) and depleted oil and gas reservoirs (e.g., Dance 2013; Underschultz et al. 2011; Vidal-gilbert et al. 2010; Dance et al. 2009).

The risk of leakage of injected CO<sub>2</sub> in geological media through leaky faults or abandoned wells is a concern (Bagheri et al. 2018; Busch et al. 2010; Michael et al. 2010), particularly in the short-term when injected CO<sub>2</sub> has not been immobilized. However, as Alcalde et al. (2018) mentioned the amount of CO<sub>2</sub> lost would probably be small as various trapping mechanisms are involved in the CO<sub>2</sub> storage process in order to guarantee CO<sub>2</sub> storage security and integrity. These mechanisms include: capillary or residual trapping (e.g., Ni et al. 2019; Rasmusson et al. 2018; Raza et al. 2017; Al-khdheewi et al. 2017; Krevor et al. 2015; Burnside and Naylor 2014; Krevor et al. 2012; Pentland et al. 2011; Krevor et al. 2011; Juanes et al. 2006; Kumar et al. 2004), dissolution trapping (e.g., Soltanian et al. 2017; Ranganathan et al. 2012; Iglauer 2011; Espinoza et al. 2011; Özgür 2006; Riaz et al. 2006; Ennis-king et al. 2005; Xu and Chen 2006), mineral trapping (e.g., De Silva 2015; Gao et al. 2013; Gaus 2010) and structural trapping (e.g., Ahmadinia et al. 2019). The latter is most often adopted, whereby impermeable seals (e.g., clayey shale and silty shales) with high capillary pressure acts as a barrier to buoyant fluids (e.g., Iglauer 2018; Wollenweber et al. 2010), and fluids accumulate as a result of the geometric configuration of rocks (Biddle and Wielchowsky 1994), known as traps. Along with structural traps (folds and/or faults), stratigraphic traps, where variations in local stratigraphy trap fluids, can create an effective mechanism (Shariatipour et al. 2016a). Although stratigraphic traps are variously classified, they are characterized by their association (or not) with unconformities (Rittenhouse 1972). The ones associated with unconformities can be grouped as above or below unconformities. Traps that are not in contact with unconformities can be termed primary (depositional) or secondary (diagenetic). In the oil and gas industry, traps that are adjacent to unconformities can form large stratigraphic traps (e.g., East Texas field, USA (Halbouty 1991), Prudhoe Bay, USA (Specht et al. 1986), and Bell Creek Field, USA (McGregor and Biggs 1968)). Primary or depositional traps include buried depositional relief such as carbonate reef and submarine fan deposits (e.g., the Devonian reef fields, Canada (Moore 1989), Kashagan field, Caspian Basin (Ronchi et al. 2010), and the Balder oil field of the Norwegian section of the North Sea (Sarg and Skjold 1982)), facies changes (e.g., Wonsits Valley field, USA (Castle 1990), and depositional pinchouts (e.g., Redwash field, USA (Castle 1990)). These examples are among the very few giant oil accumulations associated with such traps. Another major group of stratigraphic traps are formed due to post-depositional alteration of strata (e.g., Scipio-Albion trend in Michigan,

USA (Harding 1974) (see Biddle and Wielchowsky (1994) and references herein). In the CO<sub>2</sub> storage experience, such traps can restrict the upward migration of fluids and thus influence storage security, effectiveness and capacity (Ambrose et al. 2008), and create effective storage sites (Hovorka et al. 2004).

Another important aspect to be considered in CO<sub>2</sub> storage context is fluids flow within a reservoir which is linked to its depositional environment (Okwen et al. 2014). Depositional environment determines the sediment distribution, grain size and sorting (Bjørlykke 2014), and thereby petrophysical properties and reservoir quality. The shallow-marine environments are defined as depositional environments that lie between the influence of marine and continental processes (Stow et al. 1996). They formed reservoirs in many of the world's major hydrocarbon provinces (Howell et al. 2008) and have high storage efficiency (Okwen et al. 2014) as sediment was deposited in relatively high energy environments and exhibit good sorting and high porosity (Bjørlykke 2014). Shallow marine reservoirs are being used or considered for industrial storage or test sites, include the: In Salah CO<sub>2</sub> storage project (Ringrose et al. 2013; Iding and Ringrose 2010), Captain Sandstone (Jin et al. 2012), the CO<sub>2</sub>CRC Otway Project (Dance 2013), and Frio Formation (Hovorka et al. 2004). The Sleipner project in Norway is an excellent stratigraphic trap used for the geological storage of CO<sub>2</sub>, where CO<sub>2</sub> is injected into the Utsira Formation, a shallow marine sequence. CO<sub>2</sub> is partially trapped beneath nine, relatively impermeable, intra-reservoir mudstone layers situated beneath the main caprock (Chadwick et al. 2008; Bickle et al. 2007), as depositional environments provide reservoir and seal combinations (stratigraphic trap) that can store CO<sub>2</sub> effectively.

The importance of realistic geological modelling to reduce the risks and uncertainties associated with CO<sub>2</sub> storage in geological media has long been acknowledged (Pourmalek et al. 2021; Newell et al. 2019; Pourmalek and Shariatipour 2019; Newell and Shariatipour 2016; Shariatipour et al. 2016b, 2016a; Ashraf 2014; Ghanbari et al. 2006; Hovorka et al. 2004). The modelling of complex heterogeneity in subsurface permeability, controlled by sedimentary facies and diagenesis is difficult; however, it is a critical step in identifying uncertainties in fluid flow, storage capacity and security within stratigraphic traps (Ashraf 2014; Lengler et al. 2010; Ambrose et al. 2008; Flett et al. 2007). A detailed understanding of facies can be achieved by using outcrop analogue to construct realistic 3D reservoir models (Howell et al. 2014; Barnaby and Ward 2007). Analogue reservoir models were previously used to simulate and investigate the effects of reservoir architecture on fluid movement (e.g., Zuluaga et al. 2016; Wilson et al. 2011; Rotevatn et al. 2009; Sharp et al. 2006; Brandsæter et al. 2005). The application of analogues in the study of subsurface CO<sub>2</sub> storage has also been studied (Newell et al. 2019; Newell and Shariatipour 2016).

In this paper we aim to systematically model three different outcrops, each representing a mixed shallow marine system with varying heterogeneity that may form a small or large stratigraphic trap and be suitable for CO<sub>2</sub> confinement. The impact of mixed facies on CO<sub>2</sub> storage is relatively poorly known but may be an important factor in many target formations. The three 3D models are based on the: 1. Grayburg Formation (US), which displays spatial

permeability linked to variations in the mixture of siliciclastic–carbonate sediments that range from < 10 percent to > 90 percent quartz sand; 2. Lorca Basin outcrop (Spain), which demonstrates the interfingering of clastic and carbonate facies, and 3. Bridport Sand Formation outcrop (UK), an example of a layered reservoir, which has thin carbonate-cemented horizons. This study will deduce whether such complex systems can act as stratigraphic traps and allow the safe geological storage of CO<sub>2</sub>.

## **1.2 Mixed Clastic-Carbonate systems**

Numerous clastic-carbonate shallow marine sequences can be found globally in both modern and ancient sequences (Tucker 2003; Mount 1985). These systems are comprised of both terrigenous siliciclastic sediment and transported or *in-situ* carbonates (Zecchin and Catuneanu 2017; Mount 1985). This mixed depositional system displays transition between those that are entirely siliciclastic and those that are entirely carbonate (Zecchin and Catuneanu 2017).

A high flux of siliciclastic sediments into a marine environment generally has a negative effect on carbonate production and the two facies are often segregated (Catuneanu et al. 2011). However, there are a number of processes that may bring them into contact, including: transport and mixing of siliciclastic and carbonate sediments due to rare, extreme events (e.g., storms); the biogenic production of carbonate on siliciclastic substrates, and sediment mixing along faulted or other high-relief marine margins where continental and marine environments interact (Mount 1985). Important interactions between siliciclastic and carbonate deposits may also continue beyond the primary depositional phase into burial diagenesis, when even a small proportion of carbonate may induce widespread cementation and porosity reduction in siliciclastic rocks (Bryant et al. 1988).

Geological formations composed of both siliciclastic and carbonate deposits can exhibit spatiotemporal facies variability, where facies occupy discrete but coeval belts or vary through geological time. High-frequency fluctuations in relative sea-level, climate or sediment supply can alternate siliciclastic or carbonate-rich sedimentation (Zecchin and Catuneanu 2017). For example, carbonate facies will often dominate during the transgressive systems tracts (TST) when large areas of the continental margin are brought into a zone of high carbonate productivity, while continental clastics dominate after a highstand and during a subsequent falling-stage systems tract (FSST) (Catuneanu et al. 2011).

Mixed siliciclastic and carbonate formations can show great variability in lithofacies, from carbonate grainstone to quartz sandstone (Barnaby and Ward 2007; Bryant et al. 1988). Studying the effects of these facies on fluid distribution is important, as they have unique petrophysical qualities (Lucia 2007).

Lateral and vertical heterogeneities resulting from mixed deposits may form baffles and barriers that influence flow behaviour (Chiarella et al. 2017) and may form stratigraphic traps as alternating carbonate and sandstones layers, with contrasting permeability, could result in reservoir and non-reservoir intervals (McNeill et al. 2004). Heterogeneity in such systems can occur from bed to lithofacies to stratigraphic scales (cm to km) (Chiarella et al. 2017; Tucker

2003). However, in this study, only stratigraphic scale was considered. Due to computational limitations finer scales were ignored. Furthermore, these systems can show scale-independent similarities (Chiarella et al. 2017).

### 1.3 Introduction to the case studies

Three case studies were selected, displaying different styles of carbonate-siliciclastic mixing. Examples were from cyclic interbedding, the interaction of carbonate and siliciclastic environments along a ‘steep’ continental-marine margin and from storm mixing.

#### Section 1 – Grayburg Formation: cyclically interbedded

The Permian Basin is a major hydrocarbon producing area in the US. The Grayburg Formation (Late Permian) of the Permian Basin is a shallow marine mixed siliciclastic-carbonate sequence displaying significant heterogeneity due to the cyclical interbedding of different lithofacies (Parker 2013; Barnaby and Ward 2007; McNeill et al. 2004) (Figure 1). This formation is subject to enhanced oil recovery (EOR) via waterflooding and gas injection and the non-reservoir equivalent is considered for wastewater disposal (He et al. 2019). The mixed carbonate and siliciclastic rocks were categorised into seven end-member lithofacies: six carbonate lithofacies (from packstone-wackstone to ooid grainstone) and one siliciclastic lithofacies (quartz sandstone) (Barnaby and Ward 2007). Finer siliciclastics, such as claystone and siltstone, do not occur.

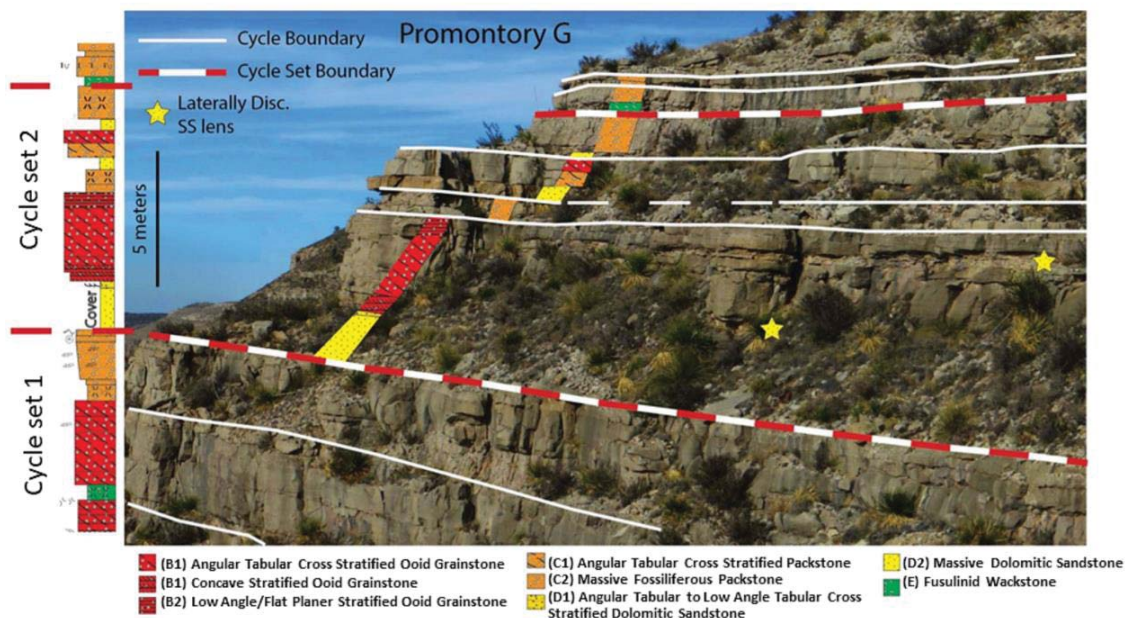


Figure 1: Outcrop photo of Grayburg Formation showing major facies (Parker 2103).

## Section 2 – Lorca Basin: steep marine margin

The Tortonian (Late Miocene) Parilla Formation of the Lorca Basin, Spain, exhibits siliciclastic-dominated, mixed siliciclastic-carbonate, and carbonate-dominated cycles. The mixed cycles developed at mid-ramp bordering an alluvial fan system (Thrana and Talbot 2006). Alluvial deposits interfinger with marginal marine and carbonate ramp facies and offer a good record of sea-level change (Figure 2). The Lorca Basin outcrop has been chosen as it exemplifies the heterogeneity of interfingering siliciclastic and carbonate facies.

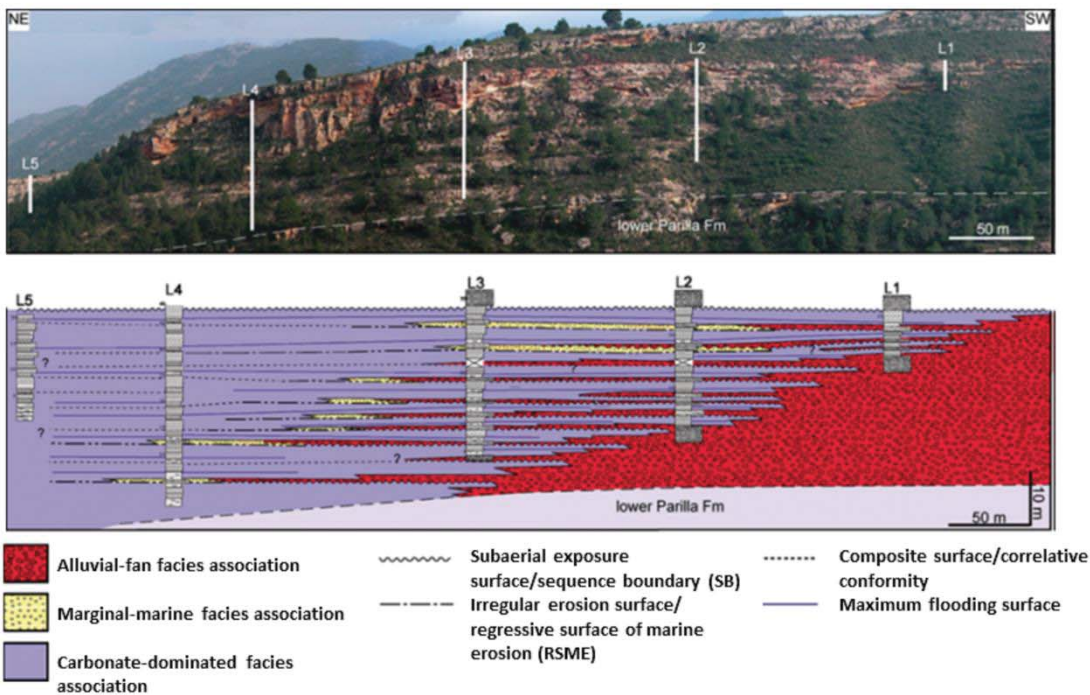


Figure 2: Outcrop photo and Miocene stratigraphy of the Lorca Basin (Thrana and Talbot 2006). The Parilla formation comprises alluvial deposits that grades into and interfingers with the marginal-marine and carbonate ramp facies.

## Section 3 – Bridport Sand Formation: storm mixing

The early Jurassic Bridport Sand Formation outcrops at Bridport on the Dorset coast of southern England, UK, and is a reservoir at the onshore Wytch Farm field (Hampson et al. 2014). The outcrop offers an appropriate analogue for several Jurassic oil and gas fields in the North Sea where thin carbonate-cemented horizons compartmentalise shallow marine sandstones (Bryant et al. 1988; Kantorowicz et al. 1987). The formation is strongly bioturbated sandstone and forms part of the mixed siliciclastic-carbonate shallow marine system (Morris et al. 2006). Permeability heterogeneity arises from preferential cementation of bioclast-rich, clay-poor sediments (Bryant et al. 1988). The distribution of the carbonate sediment, which is continuous within friable sands, may act as an extensive barrier, while the discontinuous cemented horizon can act as local baffles to fluid flow (Morris et al. 2006).

The Bridport Sand Formation is overlain by Inferior Oolite limestone and is in turn overlain by the lower Fuller's Earth. Towards the top of this sequence, the frequency of cemented horizons increases and their thickness decreases (Bryant et al. 1988) (Figure 3). Similar extensive cement horizons that are not exhumed exist in the subsurface (Bryant et al. 1988).

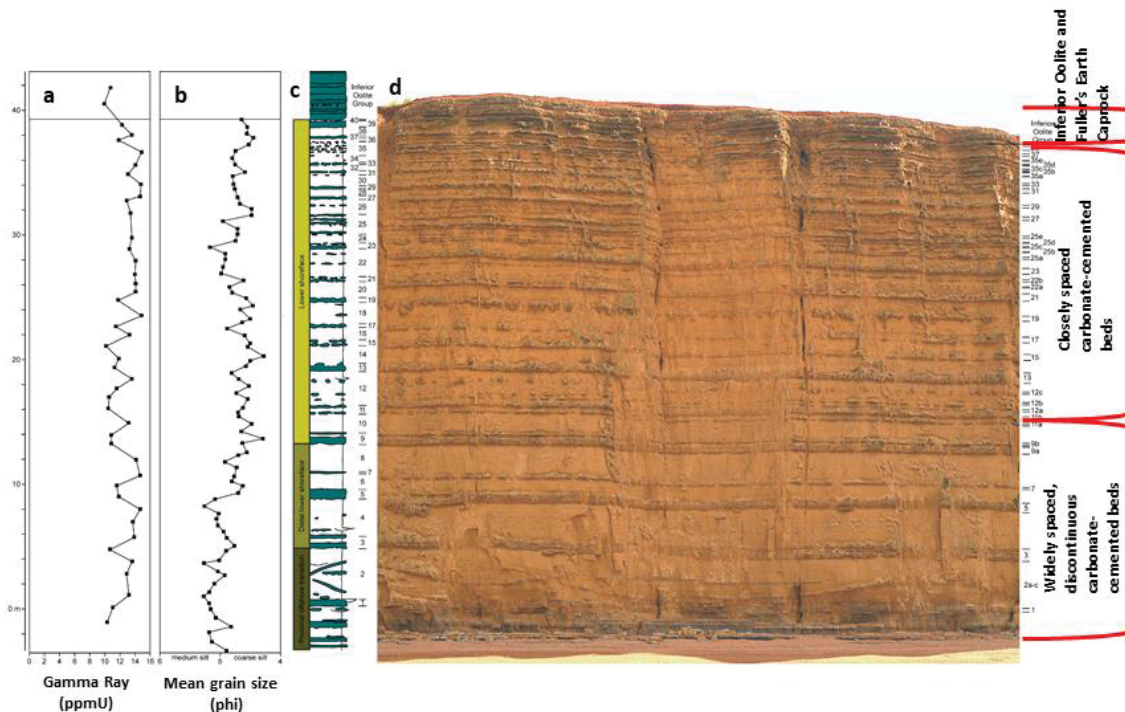


Figure 3: Bridport Sand Formation: (a) Outcrop gamma-ray profile; (b) mean grain size data; (c) lithology and interpreted facies (cemented bands is in teal); (d) and outcrop photo of Bridport Sand Formation showing Inferior Oolite, closely spaced carbonate-cemented beds and widely spaced, discontinuous carbonate-cemented beds (modified after Hampson et al. 2014).

## 2. Methodology

To meet the aim of this study, static geological models were generated in Schlumberger's Petrel software. The static models were based largely on published information (Barnaby and Ward 2007; Thrana and Talbot 2006; Bryant et al. 1988) with new observations from outcrop laser scans in the case of the Bridport Sand Formation. Dynamic modelling studies were conducted using ECLIPSE 300 with the CO2STORE module. This study assumes no conductive faults, nor leaky wellbores in the formation. Possible convection-dissolution processes were also not modelled.

### 2.1 Static models

The 3D geological models were constructed as closed aquifers assuming that intact, unfaulted regionally extensive low permeability shale layers exist below and above the models. Lateral boundaries were also closed to flow and, therefore, the pressure build-up constrains capacity (Mathias et al. 2011). Each model was uniformly gridded in the three main dimensions.

## *Section 1 – Grayburg Formation*

Six major carbonate lithofacies, from low porosity and permeability packstone-wackstone to high porosity and permeable ooid grainstone and one coarse grain siliciclastic lithofacies are recognised in the Grayburg Formation (Parker 2013; Barnaby and Ward 2007). The model is a simplified version of the Grayburg Formation outcrop (Figure 1) using carbonate and siliciclastic lithology percentages based on the study of Barnaby and Ward (2007), where quartz sand fraction can range from < 10 percent to > 90 percent (Figure 4a).

Models had spatial dimensions of 1000m×1000m×100m, which was discretized into a total of 200,000 active cells (100×100×20). Sequential indicator simulation (SIS) which is a geostatistical technique has been used here to generate the facies' distribution. This method is mainly applied where the shape of the bodies is uncertain. To test the impact of varying ratios of sandstone to carbonate on flow distribution and storage security, nine models were considered (Figure 4b), from 10 percent sandstone to 90 percent sandstone (i.e., 10:90... 90:10). These values were assigned manually. The variogram type used here was exponential with the nugget of 0.01. Range which is the maximum distance which sample values are dependent on each other was assigned 1000 in major horizontal direction, 1000 in minor direction normal to the major and 0 in vertical direction. The azimuth which is the orientation of the major direction and dip were assigned 0. Two additional models, one pure carbonate and one sandstone, were also constructed. Unlike the deterministic method which present only one model of the reservoir, stochastic methods can provide unlimited possibilities or “realisations”. Choosing the best realisation for flow modelling is the key to predicting flow movement within a reservoir; however, for the purpose of this study, these scenarios seem sufficient. Figure 4a shows the static models from the pure sandstone and carbonate scenarios, and variable sandstone and carbonate percentages. For each realisation, three models with three different carbonate petrophysical properties (Bennion and Bachu 2010), but the same sandstone petrophysical properties (Bennion and Bachu 2008), were input for the flow simulation (Table 1). 31 models were constructed. The carbonate are generally more complex than the siliciclastic rocks (e.g., Ahr 2011; Lucia 2007); consequently, the values for the sandstone facies were kept unchanged for all models. The Viking sandstone studied by Bennion and Bachu (2008; 2006b; 2006a; 2005) was used herein - a clean sandstone that exhibits a unimodal pore size distribution. Three carbonates with varying properties were used in this study, the:

1. Wabamun carbonate - a low permeability succession with a unimodal pore size distribution with few macropores (Bennion and Bachu 2010). Its high threshold capillary pressure is due to the preponderance of micropores and thus, it is assumed that these facies can act as a barrier to flow and add to storage capacity and security, forming a stratigraphic trap.
2. Nisku carbonate - a homogenous matrix, resulting in a uniform and less concentrated flow, with the assumption that it can boost effective sweep.

3. Redwater Leduc Reef carbonate - categorised as a high permeability carbonate in Bennion and Bachu (2010) and was assumed to be suitable for CO<sub>2</sub> storage as it has a higher pore volume (Table 1).

The contrast in permeability between the carbonate and sandstone in Model 1 is approximately four orders of magnitude with a transmissibility of 0.00077 cP.m<sup>3</sup>/day/bars for the carbonate facies. In Model 2 it is less than one order of magnitude with transmissibility of 1.9612 cP.m<sup>3</sup>/day/bars for the carbonate facies while in Model 3 it is 0.18 order of magnitude with transmissibility of 15.221 cP.m<sup>3</sup>/day/bars for the carbonate facies. The standardized transmissibility of sandstone is 9.9340 cP.m<sup>3</sup>/day/bars.

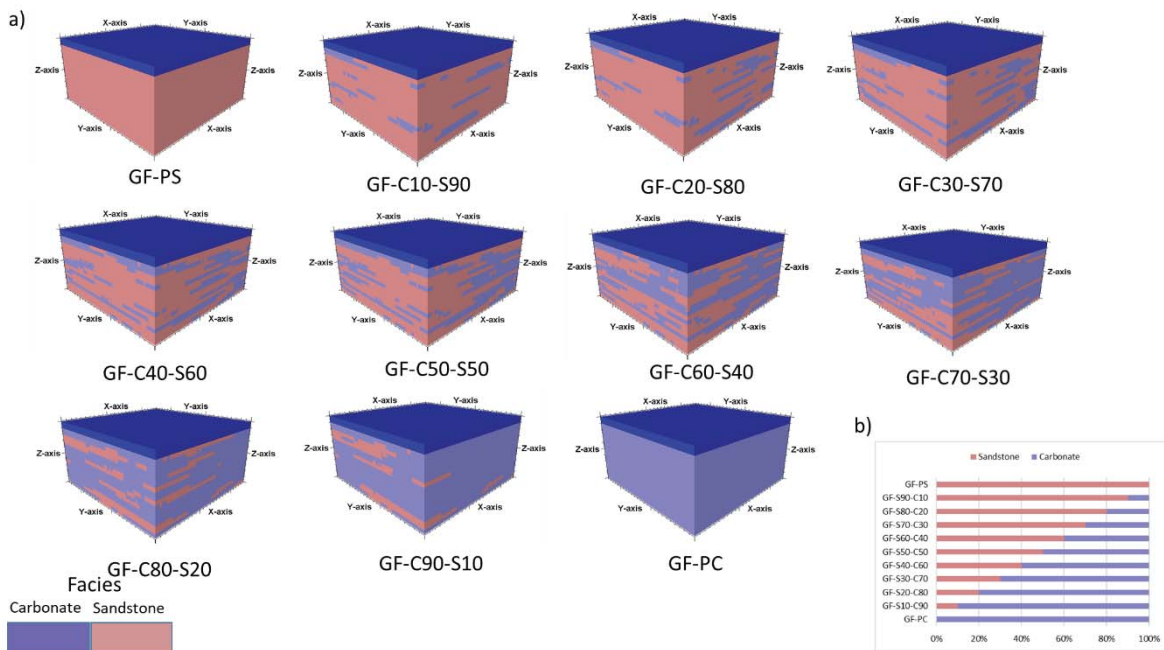


Figure 4: (a) static reservoir models (1000m×1000m×100m) from pure sandstone (GF-PS), varying ratio of carbonate to sandstone, and pure carbonate (GF-PC). GF refers to Grayburg Formation, C to carbonate and S to sandstone; (b) the percentage of each facies in each model is denoted by a number, for example the case GF-10S-90C is a model with 10 percent sandstone and 90 percent carbonate.

## Section 2 – Lorca Basin

The static geological model was constructed to capture the interfingering of carbonate and alluvial clastic facies (Figure 5) as seen at the outcrop (Figure 2) (Thrana and Talbot 2006). Such a system does not contain closed compartments. The model had dimensions of 1000m×1000m×40m discretised into 195,000 active cells (50×50×78). A Truncated Gaussian Simulation was used to generate the transitional and interfingering contact between the two facies. For comparative purposes, one homogenous sandstone model (LB-PS) was also used for flow simulation. The petrophysical properties of this mixed system are not available, therefore, the input values were taken from Table 1.

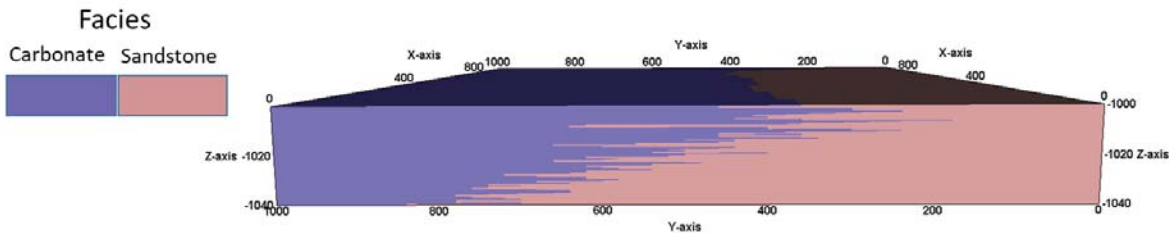


Figure 5: Static model (1000m×1000m×40m) of the Lorca Basin was constructed based on outcrop image (Figure 2) showing the interfingering of siliciclastic and carbonate facies.

### Section 3 – Bridport Sand Formation

A laser scan of the Bridport outcrop in Dorset (Figure 3) was used to construct static models (Figure 6). Although four types of cementation were recognised at the Bridport outcrop (Bryant et al. 1988), only laterally extensive sheets, which are continuous in three dimensions, were considered for flow simulation. A detailed study of fractures was ignored due to the limited grid resolution. Furthermore, these fractures are cemented and are mostly limited to the cemented bands (Bryant et al. 1988) and therefore, probably not act as avenues for flow. In contrast to the example of Lorca Basin where facies interfingered at the mid-ramp, the cemented layers in the Bridport Sand Formation compartmentalise the formation at the outcrop. The model had dimensions of 2100m×2100m×60m discretised into 588,000 active cells (70×70×120). Five models were constructed for the first part of the study, which were smaller than the 5 km coastal outcrop due to computational limitations. In each model, number of cemented horizons were modelled based on their location as observed in the laser scanned image. The 3D extent of cemented layers in four of the models (BPS-1, BPS-2, BPS-3, and BPS-4) was 90%, 70%, 50% and 10%. As only 61% of the cemented layers at the outcrop extended over 90% of the coastal outcrop, a model with cemented horizons of varying extent was also considered, one which more closely matched that observed at the Bridport outcrop (BPS-5). The permeability and porosity of the sands and cemented horizons are summarized in Table 2.

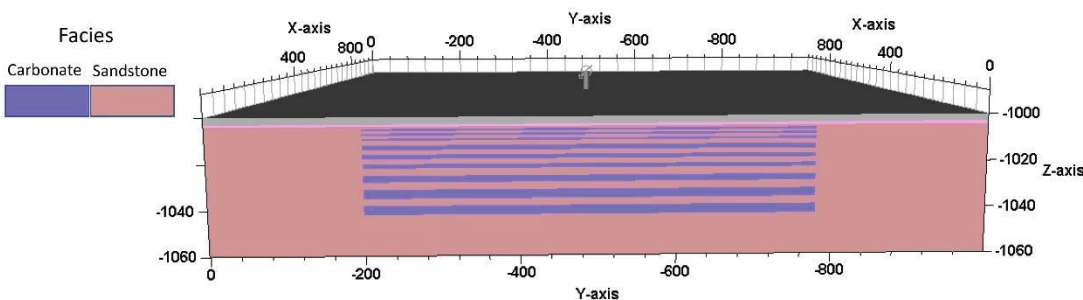


Figure 6: Static models (2100m×2100m×60m) of Bridport Sand Formation were constructed based on the laser-scanned image (Figure 16d). Towards the top of this sequence, the frequency of cemented horizons increases and their thickness decreases. The 3D extent of

cemented layers was 90%, 70%, 50% and 10% of the model. Here only the model BPS-2 with 70% cemented layers is shown.

This research was designed to examine the impact of stratigraphic variability within mixed carbonate and siliciclastic formations and thus no conductive faults, fractures or leaky wellbores were included in the models.

## 2.2 Flow simulation

The depth of the reservoir model was set at 1000 metres with the injected CO<sub>2</sub> in the supercritical state. Dynamic modelling was conducted under an initial pressure of 10.4 Mpa (fluid density of 1.06 g/cc at a salinity of 100,240 ppm) and an isothermal condition of 42°C (using a temperature gradient of 25°C/km). It was initially assumed that the reservoir was entirely saturated with brine. The constraints for injection were that CO<sub>2</sub> must remain within the storage boundary and the injection pressure pulse was not allowed beyond the domain. In addition, although values differ between authors and basins (e.g., Goater et al. 2013; Noy et al. 2012; Moss et al. 2003; Law et al. 1996; Breckels and van Eekelen 1982), the injection pressure limit was set to 90% of the fracturing pressure for Sections 1 and 2 (Bachu 2015; Law and Bachu 1996) and 75% of the lithostatic pressure for Section 3 (Noy et al. 2012), in order to maintain geomechanical stability and avoid damaging the reservoir. The injection strategy for each section is summarised in Table 3.

The relative permeability and capillary pressure curves used in this study were based on the results of Bennion and Bachu (2010; 2008; 2006b) (Table 1 and Table 2), representing comparable facies and conditions. They provided relative water-CO<sub>2</sub> permeability data for sandstone, carbonate, shale and anhydrite rocks, which allow detailed numerical simulations of CO<sub>2</sub> injection and sequestration process (Figure 7). They showed the end-point values and shape of the capillary pressure curve attribute to pore size distribution and rock heterogeneity. No hysteresis in the relative permeability was considered in this study.

Table 1: Petrophysical and flow characteristic of the four rock samples used for flow simulation in Section 1 (Grayburg Formation) and Section 2 (Lorca Basin) (Bennion and Bachu 2010; 2008; 2006b).

	Model 1		Model 2		Model 3	
	Carbonate	Sandstone	Carbonate	Sandstone	Carbonate	Sandstone
Porosity [%]	7.9	19.7	9.7	19.7	16.8	19.7
Permeability [mD]	0.018	233	46	233	353	233
Irreducible water saturation [S <sub>wirr</sub> ]	0.59	0.423	0.33	0.423	0.66	0.57
Endpoint relative permeability to CO <sub>2</sub> at S <sub>wirr</sub> [K <sub>rCO2max</sub> ]	0.528	0.2638	0.1768	0.2638	0.0476	0.2638
Threshold capillary pressure [bar]	4.93	0.29	0.58	0.29	0.21	0.29

Table 2: Petrophysical and flow characteristic used for flow simulation in Section 3 (Bridport Sand Formation) (Bennion and Bachu 2010; 2008; 2006b; Bryant et al.1988).

	Very fine sand to coarse silt	Carbonate cement bands
Porosity [%]	30	<10
Permeability [mD]	300	Negligible
Permeability anisotropy	0.1	0.1
Irreducible water saturation [ $S_{wirr}$ ]	0.423	0.59
Endpoint relative permeability to $CO_2$ at $S_{wirr}$ [ $K_{rCO2max}$ ]	0.2638	0.528
Threshold capillary pressure [bar]	0.29	4.93

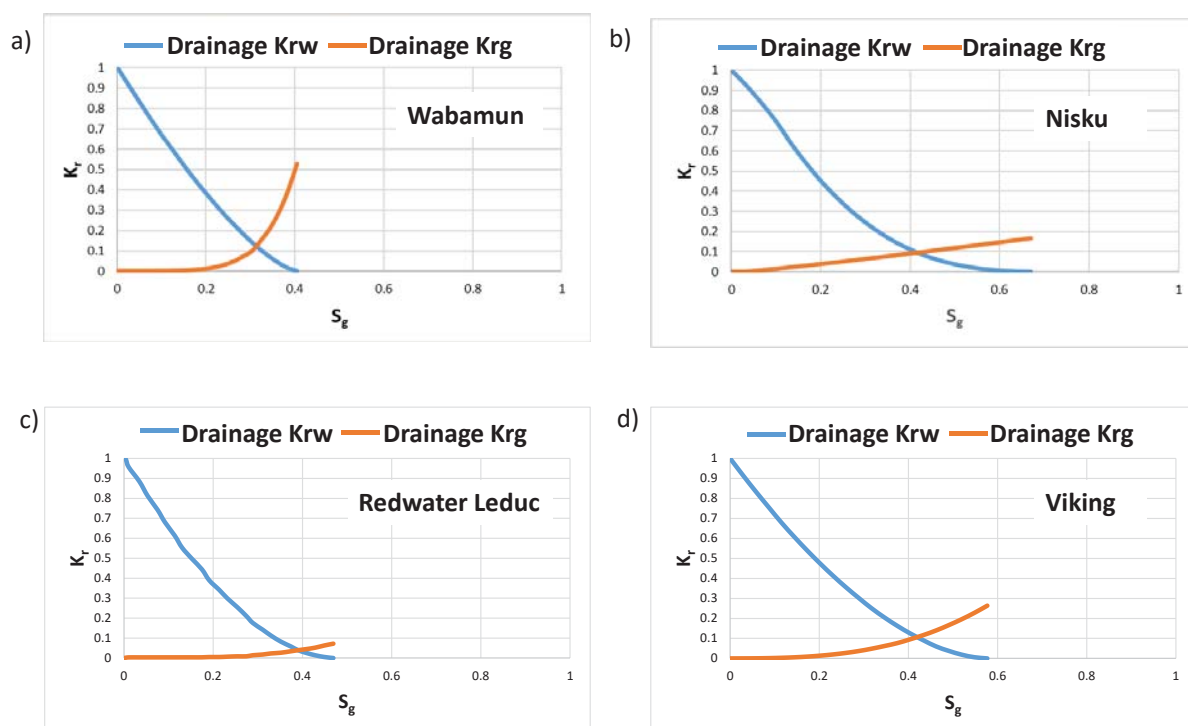


Figure 7: Relative permeability curves used throughout this study: a) Viking sandstone, b) Nisku carbonate, c) Redwater Leduc carbonate, and d) Wabamun carbonate.  $K_r$  is relative permeability ( $K_{rw}$  relative permeability for water and  $K_{rg}$  relative permeability for gas) and  $S_g$  is gas saturation.

Table 3: Injection strategy. For Bridport Sand Formation, two injection rates and two scenarios for perforation locations were considered for flow simulation.

Case	Injector location	Perforation location	Injection rate [m <sup>3</sup> /day]	Injection period [years]	Recovery period [years]
Grayburg Formation	(i=50, j=50)	(K=18-20)	9000	10	150
Lorca Basin	(i=25, j=25)	(K=34-38)	5000	10	100
Bridport Sand Formation	(i=35, j=35)	(K=95-115)	20000	10	100
		(K <sub>1</sub> =95-115; K <sub>2</sub> =93-96; K <sub>3</sub> =88-91; K <sub>4</sub> =83-86; K <sub>5</sub> =78-81; K <sub>6</sub> =73-76; K <sub>7</sub> =68-71; K <sub>8</sub> =64-66; K <sub>9</sub> =60-62; K <sub>10</sub> =56-58; K <sub>11</sub> =52-54; K <sub>12</sub> =48-50; K <sub>13</sub> =44-46; K <sub>14</sub> =40-42; K <sub>15</sub> =37-38; K <sub>16</sub> =34-35; K <sub>17</sub> =31-32; K <sub>18</sub> =28-29; K <sub>19</sub> =25-26; K <sub>20</sub> =21-23)			
		(K=95-115)	30000		

Cell location containing injector is specified using i and j in X and Y direction, respectively. K shows locations of well perforation in Z direction.

### 3. Results

#### Section 1 – Grayburg Formation

The results of models with low permeability carbonate (Wabamun Formation, Model 1) demonstrate the highest value of dissolved CO<sub>2</sub> in the water phase in models with less carbonates (Figure 8). One extensive low permeability layer (15) exists from Model GF-C20-S80 (Figure 9), consequently, the upward migration of CO<sub>2</sub> was completely restricted resulting in a plume that was not uniformly developed towards the caprock (Figure 10). The highest gas concentrations beneath the caprock, were therefore observed in the pure sandstone (GF-PS) or the model with 10 percent carbonate (GF-C10-S90-L), as CO<sub>2</sub> migration was not hindered by the low permeability carbonate layer (Figure 8).

As the percentage of carbonate facies increases, and permeability decreases, the ability of a reservoir to transmit fluid is considerably reduced. Consequently, poor levels of injectivity were observed in high percentage carbonate, and pure carbonate models (GF-C80-S20-L, GF-C90-S10-L and GF-PC-L). In these three models, very low injectivity was achieved compared to other models (e.g., 96%, 5%, and 3% of the cumulative injected gas in models GF-C80-S20-L and GF-C90-S10-L and GF-PC-L, respectively), while the maximum bottom hole pressure was reached in models GF-C90-S10-L and GF-PC-L instantaneously. In model GF-C80-S20-L, the

CO<sub>2</sub> could be injected into the reservoir until the 9th year of the injection period. Figure 11 compares the total CO<sub>2</sub> injected, the amount of dissolved CO<sub>2</sub> in the water phase, and the pressure in the model at the end of the simulation period in the pure carbonate (GF-PC-L) and pure sandstone models (GF-PS). This graph shows how rapid the bottom hole pressure limit was achieved in models with a high carbonate-sandstone ratio, resulting in injectivity issues. The optimum heterogeneity rate in models C20-S70-L and C30-S80-L makes them the most suitable configurations for CO<sub>2</sub> injection, as injection security and capacity were achieved.

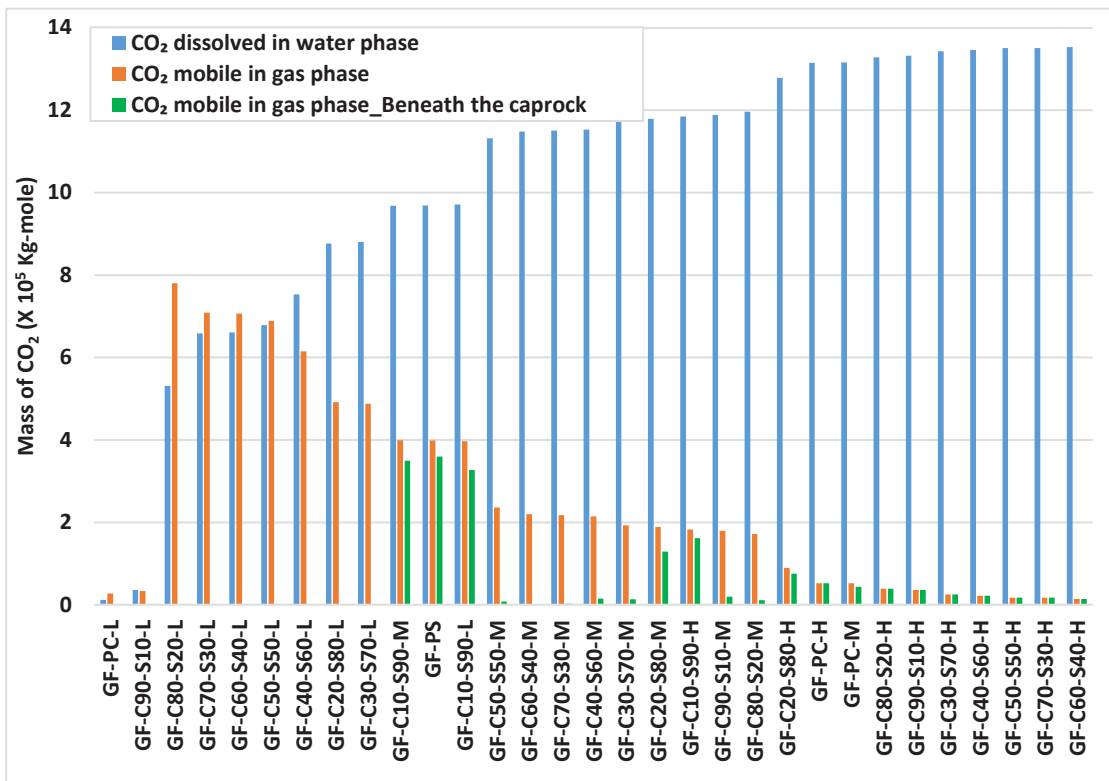


Figure 8: Dissolved and mobile CO<sub>2</sub> in the reservoir and mobile CO<sub>2</sub> beneath the caprock in all models investigated in Section 1. L, M and H refers to low, medium and high permeability carbonate facies and GF refers to Grayburg Formation. For properties see Table 1.

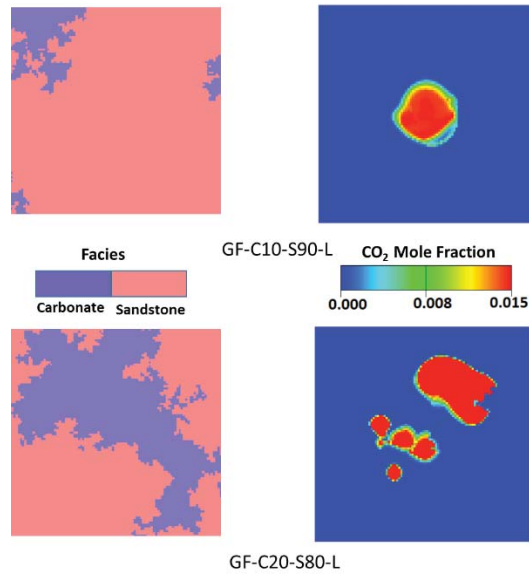


Figure 9: A low permeability layer developed across the entire model, from GF-C20-S80. This layer has been hindering the upward migration of CO<sub>2</sub> and allowing lateral migration.

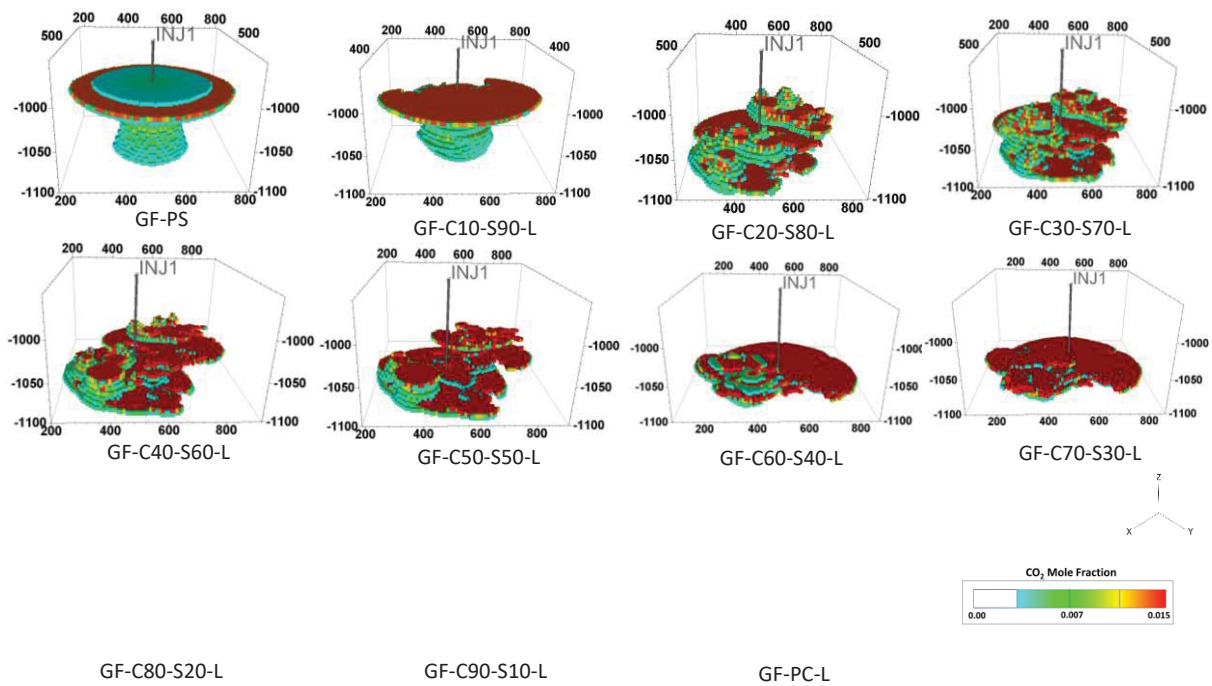


Figure 10: Flow distribution in homogeneous models (GF-PS and GF-PC-L) and models with differing carbonate and sandstone ratios. The properties of the low permeability Wabamun carbonate (L) are used for the carbonate facies in Model 1. Flow models with injectivity problem (GF-C80-S20-L, GF-C90-S10-L and GF-PC-L) are not shown. GF refers to Grayburg Formation, C to carbonate, and S to sandstone.

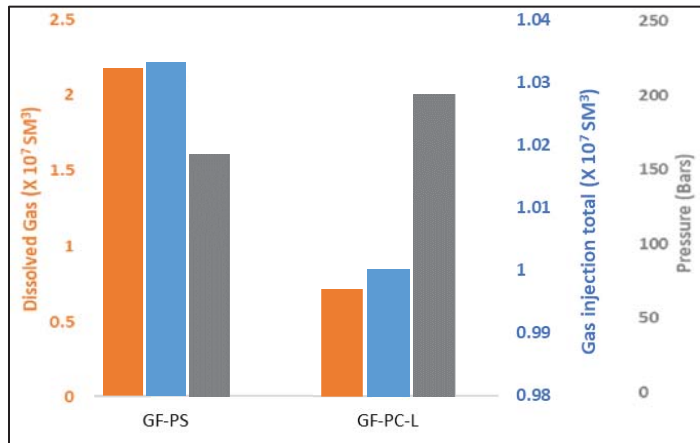


Figure 11: Average field pressure, cumulative CO<sub>2</sub> injection and amount of dissolved CO<sub>2</sub> in the water phase in the pure sandstone (GF-PS) and pure low permeability carbonate model (GF-PC-L).

The results of models with medium permeability carbonate (Nisku Formation, Model 2) demonstrates that, unlike Model 1, the injected CO<sub>2</sub> moved vertically upwards until it reached the caprock where it moved out laterally beneath it (Figure 12). The flow distribution towards the caprock was relatively symmetrical. As expected, CO<sub>2</sub> showed a uniform flow in the pure sandstone and pure carbonate models. The lateral movement of the CO<sub>2</sub> beneath the caprock was influenced by the lower permeability carbonates. The rate of dissolution trapping was highest in the homogenous, pure carbonate (GF-PC-M) model (Figure 8). In this case, the CO<sub>2</sub> plume approached a cylindrical shape around the injection well. The radius of the CO<sub>2</sub> plume around the well is smaller in the case of pure sandstone (GF-PS). The wider footprint of the CO<sub>2</sub> around the injector resulted in higher interaction between the CO<sub>2</sub> and brine and, therefore, a higher amount of CO<sub>2</sub> dissolved in the water phase. Figure 8 also shows that the volume of free gas beneath the caprock in the pure sandstone model (GF-PS) was significantly higher than for the pure carbonate model (GF-PC-M), as CO<sub>2</sub> bypassed much of the model and accumulated beneath the caprock. As a result of added heterogeneity, only small patches of free gas can be seen beneath the caprock in the heterogeneous models (e.g., GF-C50-S50-M).

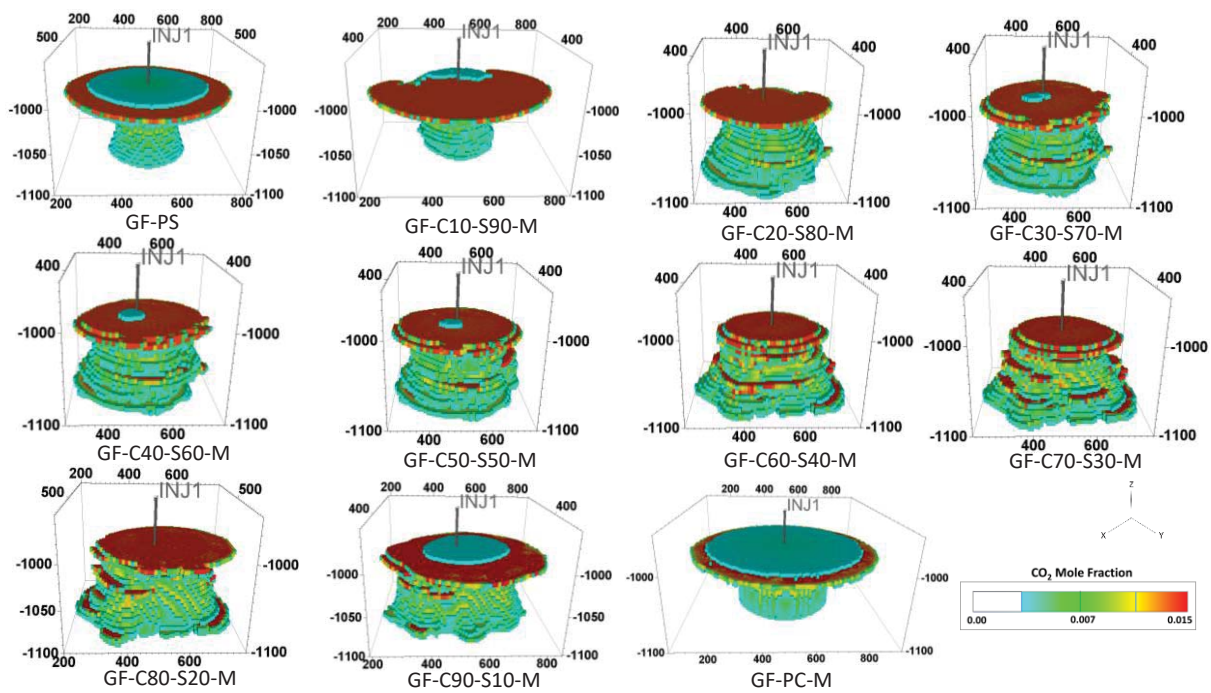


Figure 12: Flow distribution in models with different carbonate and sandstone ratios. The properties of medium permeability Nisku carbonate (M) are used for carbonate facies in Model 2. GF refers to Grayburg Formation, C to carbonate, and S to sandstone.

The results of models with high permeability carbonate (Redwater Leduc Formation, Model 3) show that the amount of dissolved  $\text{CO}_2$  in the pure sandstone model (GF-PS) was less than pure carbonate model (GF-PC-H) (**Figure 8**).  $\text{CO}_2$  reached the caprock two years earlier in the GF-PC-H compared with the GF-PS, as higher permeability in the GF-PC-H simulation facilitated migration. As the  $\text{CO}_2$  reached the caprock it again migrated laterally. As  $\text{CO}_2$  migrate further beneath the caprock in the GF-PC-H model, the interaction between these two phases was marked with more  $\text{CO}_2$  dissolved in the water phase. Therefore, the highest amount of  $\text{CO}_2$  accumulated beneath the caprock was observed in the pure sandstone model (GF-PS). The plume was less distorted compared to low permeability carbonate facies models (**Figure 13**).

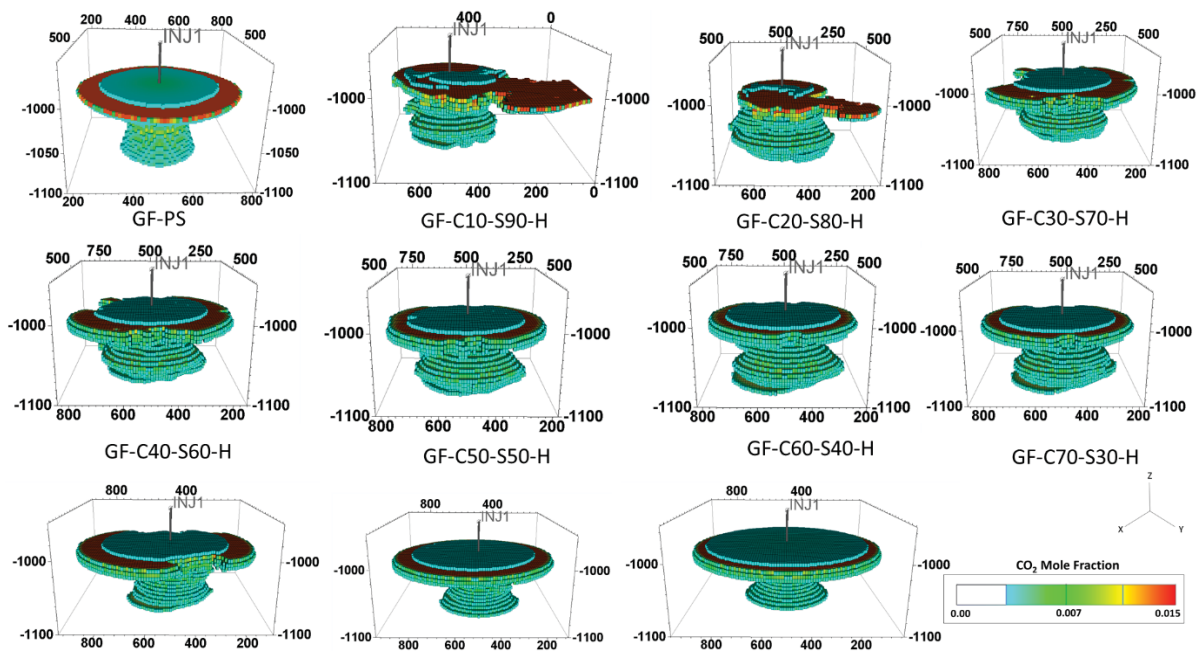


Figure 13: Flow distribution in models with differing carbonate and sandstone ratio. The properties of high permeability Redwater Leduc carbonate (H) are used for the carbonate facies in Model 3. .GF refers to Grayburg Formation, C to carbonate, and S to sandstone.

### Section 2 – Lorca Basin

The CO<sub>2</sub> distribution within the mixed interfingered system is shown in Figure 14. In these models, the plume developed asymmetrically towards the top and was completely distorted, which reflects the interaction between gravity and facies-controlled heterogeneity. The degree of plume distortion is dependent on the permeability contrast. As the heterogeneity in permeability developed across the interfingering facies, these discontinuities interrupted the vertical movement of CO<sub>2</sub>, which is retained in the lower part of Model LB-CL-S. Alternatively, most of the CO<sub>2</sub> reached the caprock in Model LB-CH-S.

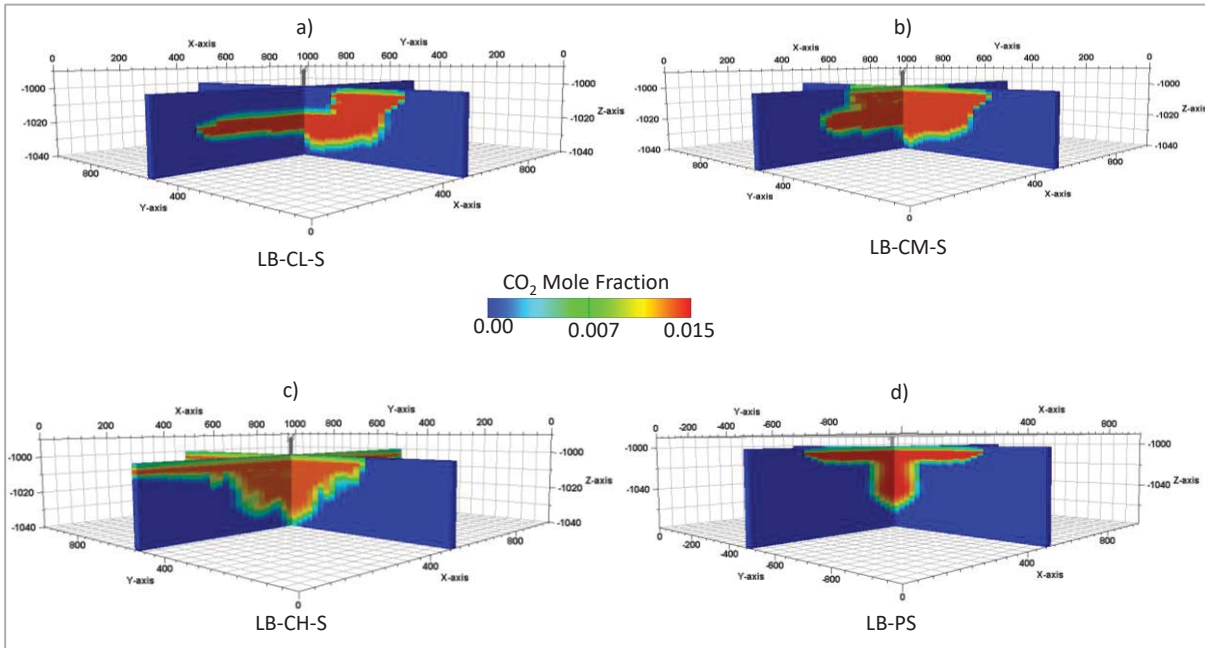


Figure 14: CO<sub>2</sub> mole fraction in the model with a) low permeability carbonate (LB-CL-S); b) medium permeability carbonate (LB-CM-S); c) high permeability carbonate (LB-CH-S); and d) homogeneous model (LB-PS). Sandstone facies properties remained constant throughout the simulation. LB refers to Lorca Basin. For properties see Table 1.

Larger amounts of mobile CO<sub>2</sub> existed beneath the caprock in the homogeneous model (LB-PS) than the high permeability carbonate facies model (LB-CH-S) (**Figure 15**). This may be the result of higher average permeability values in LB-CH-S when compared to LB-PS, and the heterogeneity of this model. This facilitated more interaction between the brine and CO<sub>2</sub>, which increased the amount of dissolved CO<sub>2</sub> in the water phase and decreased the volume of mobile gas beneath the caprock.

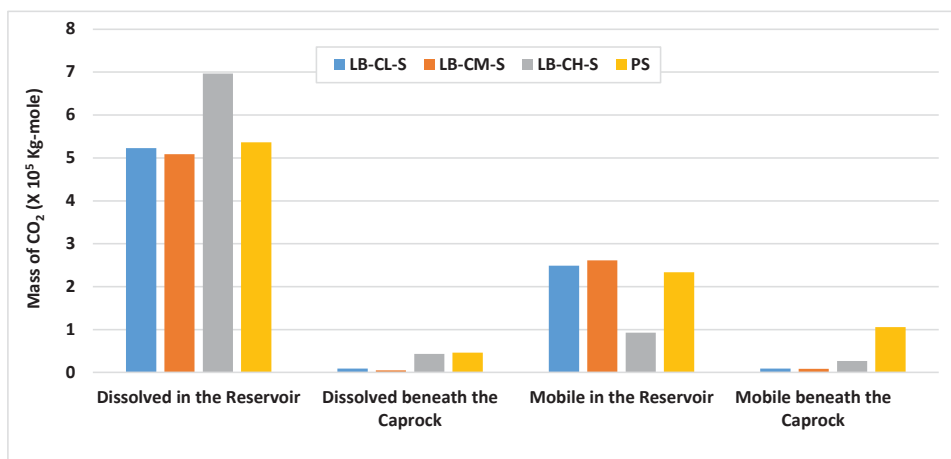


Figure 15: Dissolved and mobile CO<sub>2</sub> in the reservoir and beneath the caprock. For petrophysical and flow properties see Table 1. LB refers to Lorca Basin.

### Section 3 – Bridport Sand Formation

The CO<sub>2</sub> distribution within the Bridport Sand Formation is shown in Figure 16. The results demonstrate that the amount of mobile CO<sub>2</sub> in homogeneous models was considerable in the high permeability layer beneath the caprock compared to models with cemented horizons (Figure 17). For both injection scenarios and all models with cemented horizons, except the 10% (BPS-4), no mobile CO<sub>2</sub> occurred in the overlying Inferior Oolite. In all models CO<sub>2</sub> only partially filled the sands. In BPS-4 the injected CO<sub>2</sub> was seen to escape laterally towards the high permeability strata and the Fuller’s Earth caprock. As stated earlier, the high-density cemented fracture system was not modelled, as they are confined in well-cemented horizons (Bryant et al. 1988). It was deduced that the amount of CO<sub>2</sub> trapped as a dissolved phase is insignificantly less in models where all the sand layers were perforated.

Figure 18 demonstrates the pressure and dissolved CO<sub>2</sub> in each sand layer when the CO<sub>2</sub> was injected across the whole succession. The amount of dissolved CO<sub>2</sub> increased as the area covered by CO<sub>2</sub> increases. In the middle layers (40-42), where most coverage was observed, higher amount of dissolved CO<sub>2</sub> was seen in the water phase. However, as the sand layers thickened towards the bottom of the reservoir (e.g., 68-71), the CO<sub>2</sub> formed a narrow plume around the well, resulting in less dissolution.

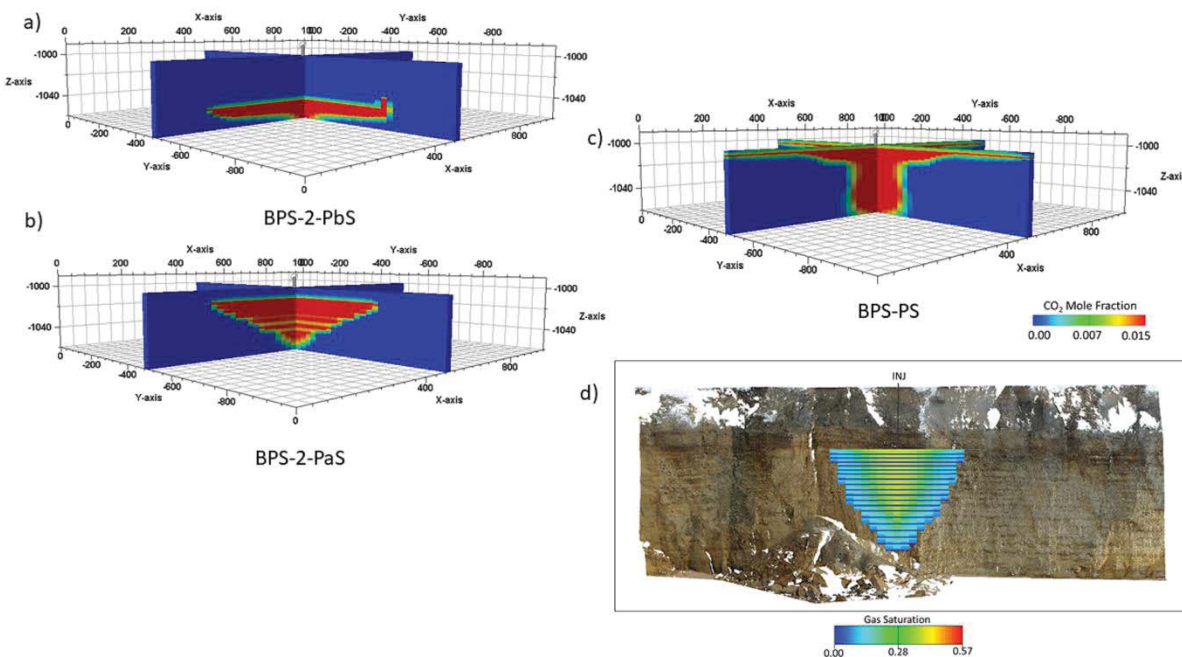


Figure 16: CO<sub>2</sub> mole fraction in the model BPS-2 with 70% cemented layers. CO<sub>2</sub> was injected through perforation; a) into the bottom-most sand layer (PbS); and b) through all sand layers (PaS). c) Homogeneous model (BPS-PS). d) Results of the Eclipse dynamic flow simulation shown on the vertical plane of the laser-scanned digital outcrop of Bridport Sand Formation that was used to build the static models. Sandstone facies properties remained constant throughout the simulation. BPS refers to Bridport Sand Formation. For properties see Table 2.

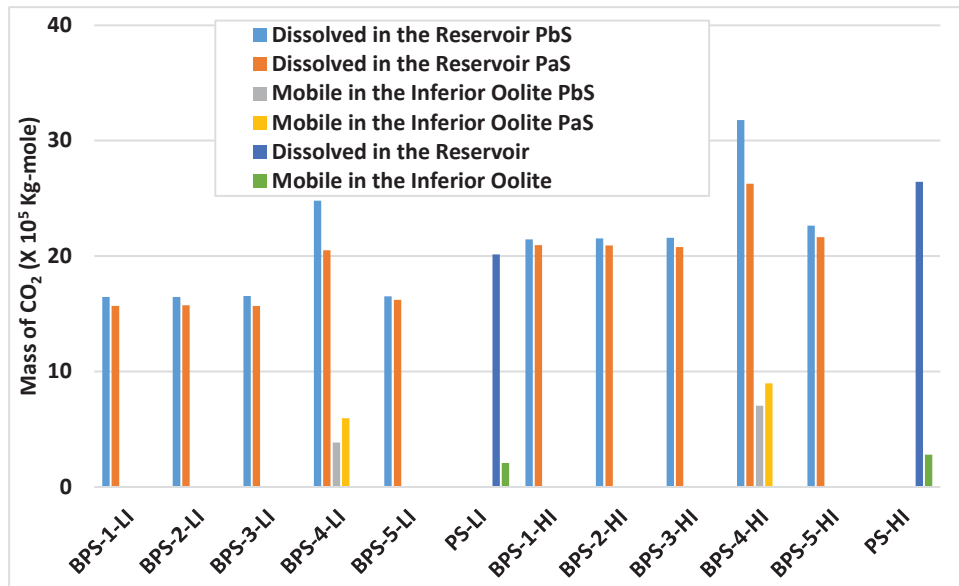


Figure 17: Dissolved CO<sub>2</sub> in the reservoir and mobile CO<sub>2</sub> in the high permeability layer (Inferior Oolite) in models with 20,000 Sm<sup>3</sup> (LI) and 30,000 Sm<sup>3</sup> injection rates (HI). In these models, CO<sub>2</sub> was injected through perforation into the bottom-most sand layer (PbS) or through all sand layers (PaS). BPS refers to Bridport sand Formation. PS-HI and PS-LI are homogeneous sandstone models with high and low injection rates, respectively. For injection strategy see Table 3.

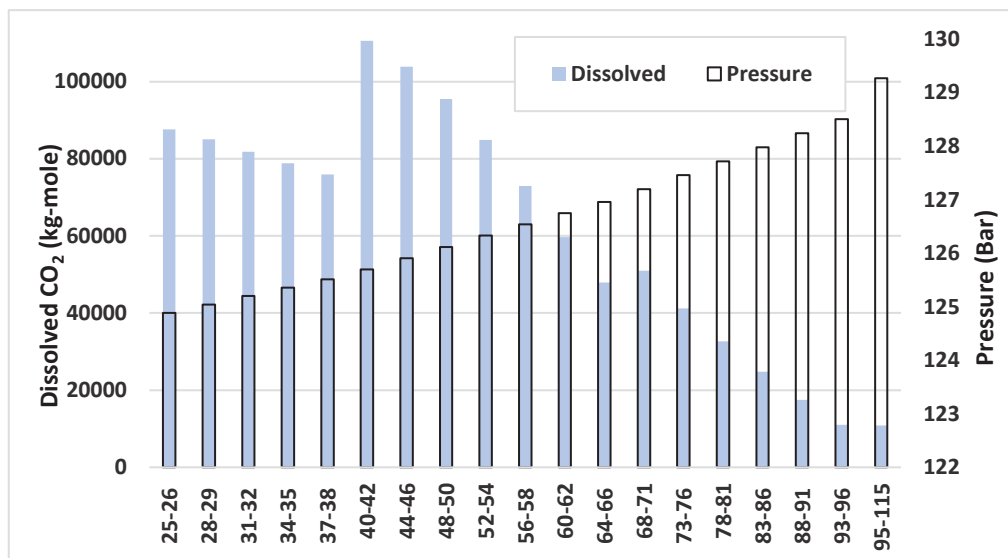


Figure 18: Dissolved CO<sub>2</sub> and the pressure in sand bands. The x-axis shows the layers where the well is open to CO<sub>2</sub> injection.

The effectiveness of mixed systems depends on a mobile gas that reaches any leakage points (i.e., transmissible faults, corroded wells or any gap in the caprock). Figure 19 compares the free gas beneath the caprock for all cases considered herein. Pure sandstone models (GR-PS, LB-PS, PBS-PS-HI and PBS-PS-LI) are the least secure scenarios. The Bridport Sand Formation

cases are the safest (except for the scenario with minimal cemented sheets) and the Grayburg Formation cases the least secure.

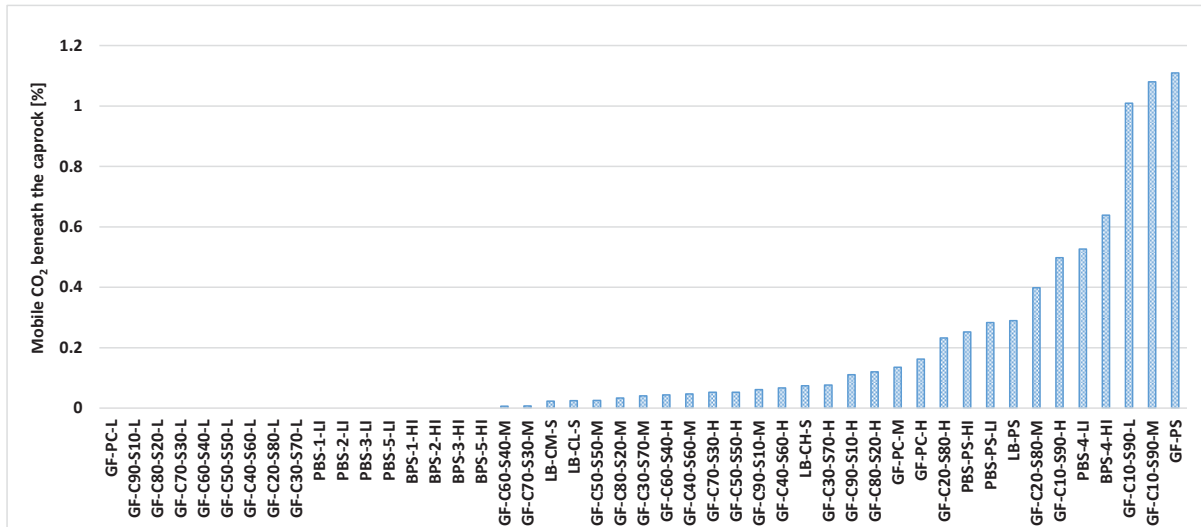


Figure 19: Percentage of free gas beneath the caprock in all cases. GF: Grayburg Formation, LB: Lorca Basin and PBS; Bridport Sand Formation.

#### 4. Discussion

##### Section 1 – Grayburg Formation

The effectiveness of CO<sub>2</sub> storage may be enhanced by sediment heterogeneity arising from the distribution of low permeability facies, as they facilitated the lateral migration of CO<sub>2</sub> which can result in longer flow paths and thus increase volume available (Goater et al. 2013; Lengler et al. 2010; Flett et al. 2007; Hovorka et al. 2004). In this study, the increase in low permeability facies did not lead to an increase in storage capacity because of a low permeability layer developed from model GF-C20-S80 (Figure 8). The reduction in available volume, storage capacity and reservoir communication are linked to the low porosity and permeability of the Wabamun carbonate facies (Section 1, Model 1). The presence of this layer was not reflected in the results of the flow simulations in Model 2 and Model 3 of the Grayburg Formation as high permeability contrast would cause considerable flow heterogeneity. The high permeability contrast (i.e., four orders of magnitude) in Model 1 affects flow so that injected CO<sub>2</sub> could not migrate vertically and instead accumulated at the bottom of the reservoir (Figure 10). This explains the irregular shaped plume in Model 1 compared to Models 2 and 3 which behave more homogeneously. In particular, low viscosity gas reservoirs are sensitive to higher contrasts in permeability and justify a simple modelling exercise (Ringrose and Bentley 2015).

Heterogeneity needs to be considered as injectivity generally decreases with increasing heterogeneity (e.g., Lengler et al. 2010) and the storage efficiency decreases with localized pressure build-up (Goater et al. 2013). Although a decrease in high permeability lithology could result in injection problems and limit CO<sub>2</sub> storage capacity, even low-permeability

aquifers can be utilized for CO<sub>2</sub> geological storage if high permeability 'sweet zones' exist close to the injector. These zones can improve injectivity and reduce reservoir pressure (Hester and Harrison 2010); alternatively a misplaced injection well may result in project failure as seen in Model 1, in scenarios with high carbonate-sandstone ratios.

In contrast, both facies in Model 2 were relatively homogenous, with a unimodal pore size distribution, uniform matrix (Bennion and Bachu 2006a; 2006c) and insignificant permeability differences (less than one order of magnitude). The injected CO<sub>2</sub> showed a relatively uniform sweep around the injection well and towards the caprock. The results in Model 2, particularly in the heterogeneous models, is driven by the small permeability differences between the two facies. The heterogeneity provided by the association of two facies can add to reservoir security. However, the reduced permeability in some parts of the reservoir, where carbonate facies delays the upward migration of the CO<sub>2</sub>, was not sufficient to completely inhibit the flow towards the caprock. Carbonate facies had considerably higher permeability values (46 mD) than typical seals (e.g., Shale=1.00E-08 mD).

The dissolved CO<sub>2</sub> in heterogeneous models was also marginally higher than in the pure carbonate scenario of Model 3, since the permeability of the carbonate facies is only 0.18 order of magnitudes higher than the permeability of sandstone facies. The lower the permeability contrast, the less irregular the plume. Although Sifuentes et al. (2009) showed that heterogeneous models had a higher CO<sub>2</sub> dissolved in the water phase and a lower mobile CO<sub>2</sub> in the reservoir, these facets depended on permeability, permeability contrast of facies, and heterogeneity rate in these models.

### *Section 2 – Lorca Basin*

In the case of Lorca Basin scenario, the CO<sub>2</sub> plume was distributed by facies discontinuities, which led to improved CO<sub>2</sub> dissolution trapping, as interfacial area has an essential role in the transfer and subsequent dissolution of CO<sub>2</sub> (Iglauer 2011). The degree of plume distortion is also dependent on the permeability contrast. The degree of interruption by these discontinuities is higher in Model LB-CL-S with low permeability carbonate, and the plume is retained in the lower part of the reservoir.

### *Section 3 – Bridport Sand Formation*

The sandstone/shale cycles offer effective confinement in hydrocarbon and CO<sub>2</sub> storage systems (e.g., Sleipner project (Chadwick et al. 2008)). In the case of the Bridport Sand Formation, the lateral continuity of these thin cemented layers will most likely have a significant impact on plume development towards the caprock and hence the volume of CO<sub>2</sub> sequestration in the layered systems. Banded carbonates can inhibit vertical CO<sub>2</sub> migration, act as a stratigraphic trap and reduce the reliance on a top seal, and thus seal failure is extremely unlikely. Consequently, the storage effectiveness of the system is dependent on the fidelity of these cemented horizons.

The flow modelling of these systems demonstrates that facies mixing and associated sediment heterogeneity have different influences on CO<sub>2</sub> storage capacity and security.

In the case of the Grayburg Formation, storage security and capacity were not controlled by heterogeneity alone but influenced by the permeability of each facies; their permeability contrast, the degree of heterogeneity and the relative permeability characteristic of the system. In the case of the Lorca Basin, heterogeneity through interfingering of the carbonate and clastic facies improved the storage security regardless of their facies permeability. For the Bridport Sand Formation, the existence and continuity of extended sheets of cemented carbonate contributed to storage security but not storage capacity.

The long-term storage security of CO<sub>2</sub> in such systems depends on the amount of free gas that reaches existing leakage points. Overall, these mixed systems contribute to the safe storage of CO<sub>2</sub> as insecure scenarios are associated with pure sandstones and carbonates or models with high sandstone-carbonate ratio. Among the three outcrops studied herein, the safest scenario is the Bridport Sand Formation, although this is dependent on the continuity of cemented layers. The least secure scenario is the Grayburg Formation as the cemented bands in Bridport Sand Formation inhibited the vertical migration of CO<sub>2</sub>. However, in the case of Grayburg Formation, heterogeneity in the models either cause the compartmentalization of the reservoir, thus reducing CO<sub>2</sub> dissolution, or allowed CO<sub>2</sub> to escape via gaps towards the caprock.

## **5. Conclusion**

In this study, three formations with differing styles of heterogeneity were explored, including variable siliciclastic and carbonate ratio, interfingering of carbonate and sand facies and a succession with narrow cemented bands. All three styles of heterogeneity are deposited within a mixed siliciclastic-carbonate system. These lithofacies, and their associated physical properties, were systematically modelled to determine how they influenced injected CO<sub>2</sub> flow, and, as such, determine their potential as stratigraphic trap for the safe geological storage of CO<sub>2</sub>.

This study has demonstrated that facies interplay and sediment heterogeneity have a varying influence on fluid flow, storage capacity and security. In the example of the Grayburg Formation storage security and capacity were not controlled by heterogeneity alone but influenced by facies permeability, permeability contrast and the relative permeability characteristic of the system. Based on the petrophysical properties of each facies, stratigraphic heterogeneity can limit connectivity and significantly increase injection pressure. In the Lorca Basin, heterogeneity achieved through the interfingering of the carbonate and clastic facies, improved the storage security regardless of their permeability. For the Bridport Sand Formation example, the existence of extended sheets of cemented carbonate contributed to storage security but not storage capacity. This study demonstrates the significance of these systems for safe CO<sub>2</sub> geological storage, as stratigraphic heterogeneity is likely be a significant feature of future storage sites. These mixed systems can minimise the large buoyancy force that act upon the top seal thus reducing the reliance of the storage security on the caprock. They can also increase the contact area between injected CO<sub>2</sub> and brine, thereby promoting CO<sub>2</sub> dissolution.

## Acknowledgement

AP would like to thank the Centre for Fluid and Complex Systems, Coventry University, UK for providing financial support for this project. The authors also wish to thank Schlumberger for the use of the ECLIPSE and Petrel software and Amarile for the use of the re-Studio. They also want to thank BGS for laser scan carried out by Lee Jones.

## List of references

- Ahmadinia, M., Shariatipour, S.M., Andersen, O., and Sadri, M. (2019) 'International Journal of Greenhouse Gas Control Benchmarking of Vertically Integrated Models for the Study of the Impact of Caprock Morphology on CO<sub>2</sub> Migration'. *International Journal of Greenhouse Gas Control* [online] 90 (July), 102802. available from <<https://doi.org/10.1016/j.ijggc.2019.102802>>
- Ahr, W.M. (2011) *Geology of Carbonate: The Identification, Description, and Characterization of Hydrocarbon Reservoirs in Carbonate Rocks*. John Wiley & Sons.
- Al-khdheewi, E.A., Vialle, S., Barifcani, A., Sarmadivaleh, M., and Iglauer, S. (2017) 'International Journal of Greenhouse Gas Control Impact of Reservoir Wettability and Heterogeneity on CO<sub>2</sub> -Plume Migration and Trapping Capacity'. *International Journal of Greenhouse Gas Control* [online] 58, 142–158. available from <<http://dx.doi.org/10.1016/j.ijggc.2017.01.012>>
- Alcalde, J., Flude, S., Wilkinson, M., Johnson, G., Edlmann, K., Bond, C.E., Scott, V., Gil, S.M. V, Ogaya, X., and Haszeldine, R.S. (2018) 'Estimating Geological CO<sub>2</sub> Storage Security to Deliver on Climate Mitigation'. *Nature Communications* [online] 1 (9), 1–13. available from <<https://doi.org/10.1038/s41467-018-04423-1>>
- Ambrose, W.A., Lakshminarasimhan, S., Holtz, M.H., Núñez-López, V., Hovorka, S.D., and Duncan, I. (2008) 'Geologic Factors Controlling CO<sub>2</sub> Storage Capacity and Permanence: Case Studies Based on Experience with Heterogeneity in Oil and Gas Reservoirs Applied to CO<sub>2</sub> Storage'. *Environmental Geology* [online] 54 (8), 1619–1633. available from <<https://doi.org/10.1007/s00254-007-0940-2>>
- Ashraf, M. (2014) 'Geological Storage of CO<sub>2</sub>: Heterogeneity Impact on the Behavior of Pressure'. *International Journal of Greenhouse Gas Control* 28, 356–368
- Bachu, S. (2015) 'Review of CO<sub>2</sub> Storage Efficiency in Deep Saline Aquifers'. *International Journal of Greenhouse Gas Control* [online] 40 (September 2015), 188–202. available from <<http://dx.doi.org/10.1016/j.ijggc.2015.01.007>>
- Bagheri, M., Shariatipour, S.M., and Ganjian, E. (2018) 'A Review of Oil Well Cement Alteration in CO<sub>2</sub>-Rich Environments'. *Construction and Building Materials* [online] 186, 946–968. available from <<https://doi.org/10.1016/j.conbuildmat.2018.07.250>>
- Barnaby R.J and Ward W. B (2007) 'Outcrop Analog for Mixed Siliciclastic – Carbonate Ramp Reservoirs — Stratigraphic Hierarchy, Facies Architecture, and Geologic Heterogeneity: Grayburg Formation'. *Journal of Sedimentary Research* [online] 77 (1), 34–58. available from <<https://doi.org/10.2110/jsr.2007.007%0A>>
- Bennion, B. and Bachu, S. (2005) 'Relative Permeability Characteristics for Supercritical CO<sub>2</sub> Displacing Water in a Variety of Potential Sequestration Zones in the Western Canada Sedimentary Basin'. *SPE Annual Technical Conference and Exhibition. Society of Petroleum Engineers*. [online] (9–12 October). available from <<https://doi.org/10.2118/95547-MS>>
- Bennion, D.B. and Bachu, S. (2006a) 'Dependence on Temperature, Pressure, and Salinity of

the IFT and Relative Permeability Displacement Characteristics of CO<sub>2</sub> Injected in Deep Saline Aquifers'. *SPE Annual Technical Conference and Exhibition. Society of Petroleum Engineers*. [online] (24–27 September). available from <<https://doi.org/10.2118/102138-MS>>

- Bennion, D.B. and Bachu, S. (2006b) 'Supercritical CO<sub>2</sub> and H<sub>2</sub>S — Brine Drainage and Imbibition Relative Permeability Relationships for Intergranular Sandstone and Carbonate Formations'. *SPE Europec/EAGE Annual Conference and Exhibition*. [online] (12–15 June). available from <<https://doi.org/10.2118/99326-MS>>
- Bennion, D.B. and Bachu, S. (2006c) 'The Impact of Interfacial Tension and Pore - Size Distribution / Capillary Pressure Character on CO<sub>2</sub> Relative Permeability at Reservoir Conditions in CO<sub>2</sub>-Brine Systems'. *SPE/DOE Symposium on Improved Oil Recovery. Society of Petroleum Engineers*. [online] (22–26 April). available from <<https://doi.org/10.2118/99325-MS>>
- Bennion, D.B. and Bachu, S. (2008) 'Drainage and Imbibition Relative Permeability Relationships for Supercritical CO<sub>2</sub> / Brine and H<sub>2</sub>S / Brine Systems in Intergranular Sandstone, Carbonate, Shale, and Anhydrite Rocks'. in *SPE Reservoir Evaluation & Engineering*. held 2008. 487–496
- Bennion, D.B. and S Bachu (2010) 'Drainage and Imbibition CO<sub>2</sub> / Brine Relative Permeability Curves at Reservoir Conditions for Carbonate Formations'. *SPE Annual Technical Conference and Exhibition. Society of Petroleum Engineers*. [online] (12–15 June), 1–18. available from <<https://doi.org/10.2118/134028-MS>>
- Benson, S.M. and Surles, T. (2006) *Carbon Dioxide Capture and Storage: An Overview with Emphasis on Capture and Storage in Deep Geological Formations*. 94 (10)
- Bickle, M., Chadwick, A., Huppert, H.E., Hallworth, M., and Lyle, S. (2007) 'Modelling Carbon Dioxide Accumulation at Sleipner: Implications for Underground Carbon Storage'. *Earth and Planetary Science Letters* [online] 255 (1–2), 164–176. available from <<https://doi.org/10.1016/j.epsl.2006.12.013>>
- Biddle, K.T. and Wielchowsky, C.C. (1994) 'Hydrocarbon Traps'. in *The Petroleum System- from Source to Trap*. vol. 60. AAPG Memoir, 219–235
- Birkholzer, J.T., Zhou, Q., and Tsang, C. (2009) 'Large-Scale Impact of CO<sub>2</sub> Storage in Deep Saline Aquifers: A Sensitivity Study on Pressure Response in Stratified Systems'. *International Journal of Greenhouse Gas Control*, [online] 3 (2), 181–194. available from <<https://doi.org/10.1016/j.ijggc.2008.08.002>>
- Bjørlykke, K. (2014) 'Relationships between Depositional Environments, Burial History and Rock Properties. Some Principal Aspects of Diagenetic Process in Sedimentary Basins'. *Sedimentary Geology* [online] 301, 1–14. available from <<http://dx.doi.org/10.1016/j.sedgeo.2013.12.002>>
- Brandsæter, I., McIlroy, D., Lia, O., Ringrose, P., and Næss, A. (2005) 'Reservoir Modelling and Simulation of Lajas Formation Outcrops (Argentina) to Constrain Tidal Reservoirs of the Halten Terrace (Norway)'. *Petroleum Geoscience* [online] 11 (1), 37–46. available from <<https://doi.org/10.1144/1354-079303-611>>
- Breckels, I.M. and van Eekelen, H.A.M. (1982) 'Relationship between Horizontal Stress and Depth in Sedimentary Basins'. *Journal of Petroleum Technology* [online] 34 (09), 2191–2199. available from <<http://www.onepetro.org/doi/10.2118/10336-PA>>
- Bryant, D., Kantorowicz, J.D., and Love, C.F. (1988) 'The Origin and Recognition of Laterally Continuous Carbonate-Cemented Horizons in the Upper Lias Sands of Southern England'. *Marine and Petroleum Geology* 5 (2), 108–133

- Burnside, N.M. and Naylor, M. (2014) 'Review and Implications of Relative Permeability of CO<sub>2</sub>/Brine Systems and Residual Trapping of CO<sub>2</sub>'. *International Journal of Greenhouse Gas Control* [online] 23, 1–11. available from <<http://dx.doi.org/10.1016/j.ijggc.2014.01.013>>
- Busch, A., Amann-Hildenbrand, A., Bertier, P., Waschbuesch, M., and Krooss, B.M. (2010) 'The Significance of Caprock Sealing Integrity for CO<sub>2</sub> Storage'. *SPE International Conference on CO<sub>2</sub> Capture, Storage, and Utilization*. Society of Petroleum Engineers. [online] (10–12 November). available from <<https://doi.org/10.2118/139588-MS>>
- Castle, J.W., 1990 (1990) 'Sedimentation in Eocene Lake Uinta (Lower Green River Formation), Northeastern Uinta Basin, Utah'. in *Lacustrine Basin Exploration: Case Studies and Modern Analogs*. 243–263
- Catuneanu, O., Galloway, W.E., Kendall, C.G.S.C., Miall, A.D., Posamentier, H.W., Strasser, A., and Tucker, M.E. (2011) 'Sequence Stratigraphy: Methodology and Nomenclature'. *Newsletters on Stratigraphy* [online] 44 (3), 173–245. available from <<http://dx.doi.org/10.1127/0078-0421/2011/0011>>
- Celia, M.A., Bachu, S., Nordbotten, J.M., and Bandilla, K.W. (2015) 'Status of CO<sub>2</sub> Storage in Deep Saline Aquifers with Emphasis on Modeling Approaches and Practical Simulations'. *Water Resources Research* [online] 51 (9), 6846–6892. available from <<https://doi.org/10.1002/2015WR017609>>
- Chadwick, A., Arts, R., Bernstone, C., May, F., Thibeau, S., and Zweigel, P. (2008) *Best Practice for the Storage of CO<sub>2</sub> in Saline Aquifers - Observations and Guidelines from the SACS and CO<sub>2</sub>STORE Projects* [online] available from <<http://nora.nerc.ac.uk/id/eprint/2959>>
- Chiarella, D., Longhitano, S.G., and Tropeano, M. (2017) 'Types of Mixing and Heterogeneities in Siliciclastic-Carbonate Sediments'. *Marine and Petroleum Geology* [online] 88, 617–627. available from <<http://dx.doi.org/10.1016/j.marpetgeo.2017.09.010>>
- Dance, T. (2013) 'Assessment and Geological Characterisation of the CO<sub>2</sub>CRC Otway Project CO<sub>2</sub> Storage Demonstration Site: From Prefeasibility to Injection'. *Marine and Petroleum Geology* [online] 46, 251–269. available from <<https://doi.org/10.1016/j.marpetgeo.2013.06.008>>
- Dance, T., Spencer, L., and Xu, J.Q. (2009) 'Geological Characterisation of the Otway Project Pilot Site: What a Difference a Well Makes'. *Energy Procedia* [online] 1 (1), 2871–2878. available from <<https://doi.org/10.1016/j.egypro.2009.02.061>>
- Ennis-King, J. and Paterson, L. (2005) 'Role of Convective Mixing in the Long-Term Storage of Carbon Dioxide in Deep Saline Formations'. *SPE* [online] 10 (03), 349–356. available from <<https://doi.org/10.2118/84344-PA>>
- Espinoza, D.N., Kim, S.H., and Santamarina, J.C. (2011) 'CO<sub>2</sub> Geological Storage – Geotechnical Implications'. *KSCE Journal of Civil Engineering* [online] 15, 707–719. available from <<https://doi.org/10.1007/s12205-011-0011-9>>
- Flett, M., Gurton, R., and Weir, G. (2007) 'Heterogeneous Saline Formations for Carbon Dioxide Disposal: Impact of Varying Heterogeneity on Containment and Trapping'. *Journal of Petroleum Science and Engineering* [online] 57 (1–2), 106–118. available from <<https://doi.org/10.1016/j.petrol.2006.08.016>>
- Gao, X., Liu, L., Jiang, Z., Shang, X., and Liu, G. (2013) 'Geoscience Frontiers A Pre-Paleogene Unconformity Surface of the Sikeshe Sag, Junggar Basin: Lithological, Geophysical and Geochemical Implications for the Transportation of Hydrocarbons'. *Geoscience*

- Frontiers* [online] 4 (6), 779–786. available from  
<<http://dx.doi.org/10.1016/j.gsf.2012.12.003>>
- Gaus, I. (2011) 'Role and Impact of CO<sub>2</sub> – Rock Interactions during CO<sub>2</sub> Storage in Sedimentary Rocks'. *International Journal of Greenhouse Gas Control* 4 (1)
- Ghanbari, S., Pickup, G.E., Mackay, E., Gozalpour, F., and Todd, A.C. (2006) 'Simulation of CO<sub>2</sub> Storage in Saline Aquifers'. *Chemical Engineering Research and Design* 84 (A9), 764–775
- Goater, A.L., Bijeljic, B., and Blunt, M.J. (2013) 'Dipping Open Aquifers — The Effect of Top-Surface Topography and Heterogeneity on CO<sub>2</sub> Storage Efficiency'. *International Journal of Greenhouse Gas Control* [online] 17, 318–331. available from  
<<http://dx.doi.org/10.1016/j.ijggc.2013.04.015>>
- Halbouty, M.T. (1991) 'East Texas Field--USA East Texas Basin, Texas.' in *Stratigraphic Traps, II*: ed. by Foster, N.H. and Beaumont, E.A. AAPG Treatise of Petroleum Geology, Atlas of Oil and Gas Fields, 189–206
- Hampson, G.J., Morris, J.E., and Johnson, H.D. (2014) 'Synthesis of Time-Stratigraphic Relationships and Their Impact on Hydrocarbon Reservoir Distribution and Performance, Bridport Sand Formation, Wessex Basin, UK'. *Geological Society, London, Special Publications* [online] 404 (1), 199–222. available from  
<<https://doi.org/10.1144/SP404.2>>
- Harding, T.P. (1974) 'Petroleum Traps Associated with Wrench Faults.' *AAPG bulletin* 58 (7), 1290–1304
- He, Y., Kerans, C., Zeng, H., Janson, X., and Scott, S.Z. (2019) 'Improving Three-Dimensional Interpretation for Reservoir Model Construction: An Example of Geostatistical and Seismic Forward Modeling of Permian San Andres Shelf – Grayburg Platform Mixed Clastic – Carbonate Strata'. *AAPG Bulletin* [online] 8 (8), 1839–1887. available from  
<<https://doi.org/10.1306/11211817244%0A>>
- Hovorka, S.D., Doughty, C., Benson, S.M., Pruess, K., and Knox, P.R. (2004) 'The Impact of Geological Heterogeneity on CO<sub>2</sub> Storage in Brine Formations: A Case Study from the Texas Gulf Coast'. *Geological Society, London, Special Publications* [online] 233 (1), 147–163. available from  
<<http://sp.lyellcollection.org/lookup/doi/10.1144/GSL.SP.2004.233.01.10>>
- Howell, J.A., Martinus, W.A., and Good, T.R. (2014) 'The Application of Outcrop Analogues in Geological Modelling: A Review, Present Status and Future Outlook'. *Geological Society, London, Special Publications* 387 (1), 1–25
- Howell, J.A., Skorstad, A., Macdonald, A., Fordham, A., and Flint, S. (2008) 'Sedimentological Parameterization of Shallow-Marine Reservoirs'. *Petroleum Geoscience* [online] 14 (1), 17–34. available from <<https://doi.org/10.1144/1354-079307-787>>
- Iding, M. and Ringrose, P.S. (2010) 'Evaluating the Impact of Fractures on the Performance of the In Salah CO<sub>2</sub> Storage Site'. *International Journal of Greenhouse Gas Control* 4 (2), 242–248
- IEA (2019) *World Energy Outlook-Executive Summary*. Paris
- Iglauer, S. (2011) *Dissolution Trapping of Carbon Dioxide in Reservoir Formation Brine – A Carbon Storage Mechanism*. ed. by Dr. Hironori Nakajima. INTECH Open Access Publisher
- Iglauer, S. (2018) 'Optimum Storage Depths for Structural CO<sub>2</sub> Trapping'. *International Journal of Greenhouse Gas Control* [online] 77, 82–87. available from  
<<https://doi.org/10.1016/j.ijggc.2018.07.009>>

- IPCC (2005) *IPCC Special Report on Carbon Dioxide Capture and Storage*. Prepared by Working Group III of the Intergovernmental Panel on Climate Change [Metz, B., O. Davidson, H. C. de Coninck, M. Loos, and L. A. Meyer [online] ed. by Metz, B., O. Davidson, H. C. de Coninck, M. Loos, and L.A.M. vol. 49. United Kingdom and New York, NY, USA: Cambridge University Press, Cambridge. available from <<http://www.ncbi.nlm.nih.gov/pubmed/20942501>>
- Jin, M., Mackay, E., Quinn, M., Hitchen, K., and Akhurst, M. (2012) 'Evaluation of the CO<sub>2</sub> Storage Capacity of the Captain Sandstone Formation'. In *SPE Europe/EAGE Annual Conference. Society of Petroleum Engineers. 4-7 June* [online] available from <<https://doi.org/10.2118/154539-MS>>
- Juanes, R., Spiteri, E.J., Orr, F.M., and Blunt, M.J. (2006) 'Impact of Relative Permeability Hysteresis on Geological CO<sub>2</sub> Storage'. *Water Resources Research* 42 (12), 1–13
- Kantorowicz, J.D., Bryant, I.D. and Dawans, J.. (1987) 'Controls on the Geometry and Distribution of Carbonate Cements in Jurassic Sandstones: Bridport Sands, Southern England and Viking Group, Troll Field, Norway'. *Geological Society, London, Special Publications* [online] 36 (1), 103–118. available from <<https://doi.org/10.1144/GSL.SP.1987.036.01.09>>
- Krevor, S., Blunt, M.J., Benson, S.M., Pentland, C.H., Reynolds, C., Al-menhali, A., and Niu, B. (2015) 'Capillary Trapping for Geologic Carbon Dioxide Storage – From Pore Scale Physics to Field Scale Implications'. *International Journal of Greenhouse Gas Control* [online] 40, 221–237. available from <<http://dx.doi.org/10.1016/j.ijggc.2015.04.006>>
- Krevor, S.C.M., Pini, R., Li, B., and Benson, S.M. (2011) 'Capillary Heterogeneity Trapping of CO<sub>2</sub> in a Sandstone Rock at Reservoir Conditions'. *Geophysical Research Letters* [online] 38 (August), 1–5. available from <<https://doi.org/10.1029/2011GL048239>>
- Krevor, S.C.M., Pini, R., Zuo, L., and Benson, S.M. (2012) *Relative Permeability and Trapping of CO<sub>2</sub> and Water in Sandstone Rocks at Reservoir Conditions*. 48 (February), 1–16
- Kumar, A., Noh, M., Pope, G.A., Sepehrnoori, K., Bryant, S., and Lake, L.W. (2004) 'Reservoir Simulation of CO<sub>2</sub> Storage in Deep Saline Aquifers'. *Society of Petroleum Engineers Journal* [online] 10 (03), 17–21. available from <<https://doi.org/10.2118/89343-PA>>
- Law, D.H. and Bachu, S. (1996) 'Hydrological and Numerical Analysis of CO<sub>2</sub> Disposal in Deep Aquifers in the Alberta Sedimentary Basin'. *Energy Conversion & Management* [online] 37 (95), 1167–1174. available from <[https://doi.org/10.1016/0196-8904\(95\)00315-0](https://doi.org/10.1016/0196-8904(95)00315-0)>
- Lengler, U., Lucia, M. De, and Kühn, M. (2010) 'The Impact of Heterogeneity on the Distribution of CO<sub>2</sub>: Numerical Simulation of CO<sub>2</sub> Storage at Ketzin'. *International Journal of Greenhouse Gas Control* [online] 4 (6), 1016–1025. available from <<http://dx.doi.org/10.1016/j.ijggc.2010.07.004>>
- Lucia, F.J. (2007) *Carbonate Reservoir Characterization: An Integrated Approach*. Springer Science & Business Media
- Mathias, S.A., González, G.J., Miguel, M. De, Thatcher, K.E., and Zimmerman, R.W. (2011) 'Pressure Buildup During CO<sub>2</sub> Injection into a Closed Brine Aquifer'. *Transport in Porous Media* [online] 89 (3), 383–397. available from <<https://doi.org/10.1007/s11242-011-9776-z>>
- McGregor, A.A. and Biggs, C.A. (1968) 'Bell Creek Field, Montana: A Rich Stratigraphic Trap'. *AAPG bulletin* 52 (10), 1869–1887
- McNeill, D.F., Cunningham, K.J., Guertin, L.A., and Anselmetti, F.S. (2004) 'Depositional Themes of Mixed Carbonate-Siliciclastics in the South Florida Neogene: Application to Ancient Deposits'. *AAPG Memoir* (3), 23–43

- Michael, K., Golab, A., Shulakova, V., Ennis-King, J., Allinson, G., Sharma, S., and Aiken, T. (2010) 'Geological Storage of CO<sub>2</sub> in Saline Aquifers-A Review of the Experience from Existing Storage Operations'. *International Journal of Greenhouse Gas Control* [online] 4 (4), 659–667. available from <<https://doi.org/10.1016/j.ijggc.2009.12.011>>
- Moore, P.F. (1989) 'Devonian Reefs in Canada and Some Adjacent Areas'. in *Reefs, Canada and Adjacent Area*. ed. by H.H.J. Geldsetzer, N.P.J. and G.E.T. vol. 13. Canadian Society of Petroleum Geologists Memoir 13, 367–390
- Morris, J.E., Hampson, G.J., and Johnson, H.O.W.D. (2006) 'A Sequence Stratigraphic Model for an Intensely Bioturbated Shallow-Marine Sandstone: The Bridport Sand Formation, Wessex Basin, UK'. *Sedimentology* [online] 53, 1229–1263. available from <<https://doi.org/10.1111/j.1365-3091.2006.00811.x>>
- Moss, B., Barson, D., Rakhit, K., Dennis, H., Swarbrick, R., Evans, D., Graham, C., Armour, A. and Bathurst, P. (2003) 'Formation Pore Pressures and Formation Waters. The Millennium Atlas: Petroleum Geology of the Central and Northern North Sea': *Geological Society (London)* 317–329
- Mount, J. (1985) 'Mixed Siliciclastic and Carbonate Sediments: A Proposed First-Order Textural and Compositional Classification'. *Sedimentology* 32, 435–442
- Newell, A.J., Pourmalek, A., Butcher, A.S., and Shariatipour, S.M. (2019) 'The Importance of Lithofacies Control on Fluid Migration in Heterogeneous Aeolian Formations for Geological CO<sub>2</sub> Storage: Lessons from Observational Evidence and Modelling of Bleached Palaeoreservoirs at Salt Wash Graben, Utah'. *International Journal of Greenhouse Gas Control* [online] 91 (December 2018), 1–17. available from <<https://doi.org/10.1016/j.ijggc.2019.102841>>
- Newell, A.J. and Shariatipour, S.M. (2016) 'Linking Outcrop Analogue with Flow Simulation to Reduce Uncertainty in Sub-Surface Carbon Capture and Storage: An Example from the Sherwood Sandstone Group of the Wessex Basin, UK'. *Geological Society, London, Special Publications* [online] 436 (1), 231–246. available from <<https://doi.org/10.1144/SP436.2>>
- Ni, H., Boon, M., Garing, C., and Benson, S.M. (2019) 'Predicting CO<sub>2</sub> Residual Trapping Ability Based on Experimental Petrophysical Properties for Different Sandstone Types'. *International Journal of Greenhouse Gas Control* [online] 86 (May), 158–176. available from <<https://doi.org/10.1016/j.ijggc.2019.04.024>>
- Noy, D.J., Holloway, S., Chadwick, R.A., Williams, J.D.O., Hannis, S.A., and Lahann, R.W. (2012) 'Modelling Large-Scale Carbon Dioxide Injection into the Bunter Sandstone in the UK Southern North Sea'. *International Journal of Greenhouse Gas Control* [online] 9, 220–233. available from <<http://dx.doi.org/10.1016/j.ijggc.2012.03.011>>
- Okwen, R., Yang, F., and Frailey, A. (2014) 'Effect of Geologic Depositional Environment on CO<sub>2</sub> Storage Efficiency'. *Energy Procedia* [online] 63, 5247–5257. available from <<https://doi.org/10.1016/j.egypro.2014.11.556>>
- Orr, F.M. (2009) 'Onshore Geologic Storage of CO<sub>2</sub>'. *Science* [online] 325 (5948), 1656–1658. available from <[10.1126/science.1175677](https://doi.org/10.1126/science.1175677)>
- Özgür, E. (2006) *Assessment of Diffusive and Convective Mechanisms during Carbon Dioxide Sequestration into Deep Saline Aquifers*. MIDDLE EAST TECHNICAL UNIVERSITY
- Parker, J.A. (2013) *Outcrop Analysis of Ooid Grainstones in the Permian Grayburg Formation, Shattuck Escarpment, New Mexico*. The University of Texas at Austin
- Pentland, C.H., El-Maghraby, R., Georgiadis, A., Iglauer, S., and Blunt, M.J. (2011) 'Immiscible Displacements and Capillary Trapping in CO<sub>2</sub> Storage'. *Energy Procedia* [online] 4,

- 4969–4976. available from <<https://doi.org/10.1016/j.egypro.2011.02.467>>
- Peters, E., Egberts, P.J.P., Loeve, D., and Hofstee, C. (2015) 'CO<sub>2</sub> Dissolution and Its Impact on Reservoir Pressure Behavior'. *International Journal of Greenhouse Gas Control* [online] 43, 115–123. available from <<http://dx.doi.org/10.1016/j.ijggc.2015.10.016>>
- Pourmalek, A., Newell, A.J., Shariatipour, S.M., Butcher, A.S., Milodowski, A.E., Bagheri, M., and Wood, A.M. (2021) 'Deformation Bands in High-Porosity Sandstones : Do They Help or Hinder CO<sub>2</sub> Migration and Storage in Geological Formations ?' *International Journal of Greenhouse Gas Control* [online] 107 (February), 103292. available from <<https://doi.org/10.1016/j.ijggc.2021.103292>>
- Pourmalek, A. and Shariatipour, S.M. (2019) 'Dependence on Temperature and Salinity Gradients and the Injection Rate of CO<sub>2</sub> Storage in Saline Aquifers with an Angular Unconformity'. *Journal of Porous Media* [online] 22 (8), 1065–1078. available from <[10.1615/JPorMedia.2019025077](https://doi.org/10.1615/JPorMedia.2019025077)>
- Ranganathan, P., Farajzadeh, R., Bruining, H., and Zitha, P.L.J. (2012) 'Numerical Simulation of Natural Convection in Heterogeneous Porous Media for CO<sub>2</sub> Geological Storage'. *Transport In Porous Media* [online] 95 (1), 25–54. available from <<https://doi.org/10.1007/s11242-012-0031-z>>
- Rasmusson, K., Rasmusson, M., Tsang, Y., Benson, S., Hingerl, F., Fagerlund, F., and Niemi, A. (2018) 'Residual Trapping of Carbon Dioxide during Geological Storage — Insight Gained through a Pore-Network Modeling Approach'. *International Journal of Greenhouse Gas Control* [online] 74 (July 2017), 62–78. available from <<https://doi.org/10.1016/j.ijggc.2018.04.021>>
- Raza, A., Gholami, R., Rezaee, R., Han, C., Nagarajan, R., and Ali, M. (2017) 'Assessment of CO<sub>2</sub> Residual Trapping in Depleted Reservoirs Used for Geosequestration'. *Journal of Natural Gas Science and Engineering* [online] 43, 137–155. available from <<http://dx.doi.org/10.1016/j.jngse.2017.04.001>>
- Riaz, A., Hesse, M., Tchelepi, H.A., and Orr, F.M. (2006) 'Onset of Convection in a Gravitationally Unstable Diffusive Boundary Layer in Porous Media'. *Journal of Fluid Mechanics* [online] 548, 87–111. available from <[doi:10.1017/S0022112005007494](https://doi.org/10.1017/S0022112005007494)>
- Ringrose, P. and Bentley, M. (2015) *Reservoir Model Design* [online] Berlin: Springer. available from <<http://link.springer.com/10.1007/978-94-007-5497-3>>
- Ringrose, P.S., Mathieson, A.S., Wright, I.W., Selama, F., Hansen, O., Bissell, R., Saoula, N., and Midgley, J. (2013) 'The In Salah CO<sub>2</sub> Storage Project: Lessons Learned and Knowledge Transfer'. *Energy Procedia* [online] 37, 6226–6236. available from <<https://doi.org/10.1016/j.egypro.2013.06.551>>
- Rittenhouse, G. (1972) 'Stratigraphic-Trap Classification: Geologic Exploration Methods.' *AAPG Memoir*
- Ronchi, P., Ortenzi, A., Spa, E., Borromeo, O., Spa, E., Claps, M., and Solution, S.G. (2010) 'Depositional Setting and Diagenetic Processes and Their Impact on the Reservoir Quality in the Late Viséan – Bashkirian Kashagan Carbonate Platform (Pre-Caspian Basin, Kazakhstan)'. *AAPG bulletin* 94 (9), 1313–1348
- Rotevatn, A., Tveranger, J., Howell, J.A., and Fossen, H. (2009) 'Dynamic Investigation of the Effect of a Relay Ramp on Simulated Fluid Flow: Geocellular Modelling of the Delicate Arch Ramp, Utah'. *Petroleum Geoscience*, [online] 15 (1), 45–58. available from <[https://doi.org/10.1144/1354-079309-779%0AAdd to Cart \(\\$35\)](https://doi.org/10.1144/1354-079309-779%0AAdd to Cart ($35))>
- Sarg, J.F. and Skjold, L.J. (1982) 'Stratigraphic Traps in Paleocene Sands in the Balder Area, North Sea'. in *The Deliberate Search for the Subtle Trap*. vol. 60054. 197–206

- Shariatipour, S.M., Pickup, G.E., and Mackay, E.J. (2016a) 'Investigation of CO<sub>2</sub> Storage in a Saline Formation with an Angular Unconformity at the Caprock Interface'. *Petroleum Geoscience* [online] 22 (2), 203–210. available from <<https://doi.org/10.1144/petgeo2015-039>>
- Shariatipour, S.M., Pickup, G.E., and Mackay, E.J. (2016b) 'Simulations of CO<sub>2</sub> Storage in Aquifer Models with Top Surface Morphology and Transition Zones'. *International Journal of Greenhouse Gas Control* [online] 54, 117–128. available from <<http://dx.doi.org/10.1016/j.ijggc.2016.06.016>>
- Sharp, I., Gillespie, P., Lønøy, A., Hydro, N., Horn, S., and Morsalnezhad, D. (2006) 'Outcrop Characterisation of Fractured Cretaceous Carbonate Reservoirs, Zagros Mts, Iran'. *International Oil Conference and Exhibition in Mexico. Society of Petroleum Engineers.* (31 August-2 September)
- Sifuentes, W., Blunt, M.J., and Giddins, M.A. (2009) 'Modeling CO<sub>2</sub> Storage in Aquifers: Assessing the Key Contributors to Uncertainty'. *spe in Offshore Europe. Society of Petroleum Engineers.* (8–11 September)
- De Silva, G.P.D., Ranjith, P. and Perera, M.S.A. (2015) 'Geochemical Aspects of CO<sub>2</sub> Sequestration in Deep Saline Aquifers: A Review'. *Fuel* [online] 155 (April), 128–143. available from <<http://dx.doi.org/10.1016/j.fuel.2015.03.045>>
- Soltanian, M.R., Amooie, M.A., Gershenzon, N., Dai, Z., Ritzi, R., Xiong, F., Cole, D. and Moortgat, J. (2017) *Dissolution Trapping of Carbon Dioxide in Heterogeneous Aquifers.* 51 (13), 7732–7741
- Specht, R.N., Brown, A.E., Selman, C.H. and Carlisle, J.H. (1986) 'Geophysical Case History, Prudhoe Bay Field'. *Geophysics* 51 (5), 1039–1049
- Stow, D.A.V., Reading, H.G. and Collinson, J.D. (1996) *Sedimentary Environments: Process, Facies and Stratigraphy.*
- Thrana, C. and Talbot, M.R. (2006) 'High-Frequency Carbonate-Siliciclastic Cycles in the Miocene of the Lorca Basin (Western Mediterranean, SE Spain)'. *Geologica Acta* [online] 4, 343–354. available from <Available online at [www.geologica-acta.com](http://www.geologica-acta.com)>
- Tucker, M.E. (2003) 'Mixed Clastic – Carbonate Cycles and Sequences: Quaternary of Egypt and Carboniferous of England'. *Geologia Croatica* [online] 56 (1), 19–38. available from <<https://hrcak.srce.hr/3789>>
- Underschultz, J., Boreham, C., Dance, T., Stalker, L., Freifeld, B., Kirste, D., and Ennis-king, J. (2011) 'CO<sub>2</sub> Storage in a Depleted Gas Field : An Overview of the CO<sub>2</sub>CRC Otway Project and Initial Results'. *International Journal of Greenhouse Gas Control* [online] 5 (4), 922–932. available from <<http://dx.doi.org/10.1016/j.ijggc.2011.02.009>>
- Vidal-Gilbert, S., Tenthorey, E., Dewhurst, D., Ennis-king, J., Ruth, P. Van, and Hillis, R. (2010) 'Geomechanical Analysis of the Naylor Field , Otway Basin , Australia : Implications for CO<sub>2</sub> Injection and Storage'. *International Journal of Greenhouse Gas Control* [online] 4 (5), 827–839. available from <<http://dx.doi.org/10.1016/j.ijggc.2010.06.001>>
- Wilson, C.E., Aydin, A., Durlflosky, L.J., Sagy, A., Emily, E., Kreylos, O., and Kellogg, L.H. (2011) 'From Outcrop to Flow Simulation: Constructing Discrete Fracture Models from a LIDAR Survey'. *AAPG Bulletin* 11 (11), 1883–1905
- Wollenweber, J., Alles, S., Busch, A., Krooss, B.M., Stanjek, H., and Littke, R. (2010) 'Experimental Investigation of the CO<sub>2</sub> Sealing Efficiency of Caprocks'. *International Journal of Greenhouse Gas Control* [online] 4 (2), 231–241. available from <<http://dx.doi.org/10.1016/j.ijggc.2010.01.003>>
- Xu, X. and Chen, S. (2006) 'Convective Stability Analysis of the Long-Term Storage of Carbon

Dioxide in Deep Saline Aquifers'. *Advances in Water Resources* 29, 397–407

Zecchin, M. and Catuneanu, O. (2017) 'High-Resolution Sequence Stratigraphy of Clastic Shelves VI: Mixed Siliciclastic-Carbonate Systems'. *Marine and Petroleum Geology* [online] 88, 712–723. available from <<https://doi.org/10.1016/j.marpetgeo.2017.09.012>>

Zuluaga, L.F., Rotevatn, A., Keilegavlen, E., and Fossen, H. (2016) 'The Effect of Deformation Bands on Simulated Fluid Flow within Fault-Propagation Fold Trap Types: Lessons from the San Rafael Monocline, Utah'. *AAPG bulletin* [online] 100 (10), 1523–1540. available from <<https://doi.org/10.1306/04151614153>>